# Developments in the measurement of $G_E^n$ , the neutron electric form factor

Donal Day
University of Virginia

October 14, 2003

## Outline

- ✳ Introduction: Formalism, Interpretation, Motivation
- ✳ Models
- ✳ Experimental Techniques

  Traditional (unpolarized beams)

  Modern (polarized beams, targets, polarimeters)
- ✳ Experiments using polarized electrons at Jefferson Lab
  - Recoil polarization
  - Beam-target asymmetry
- ✳ Outlook

## Formalism

$$\frac{d\sigma}{d\Omega} = \sigma_{\mathrm{Mott}} \frac{E'}{E_0} \left\{ (F_1)^2 + \tau \left[ 2\,(F_1 + F_2)^2 \tan^2(\theta_e) + (F_2)^2 \right] \right\}$$

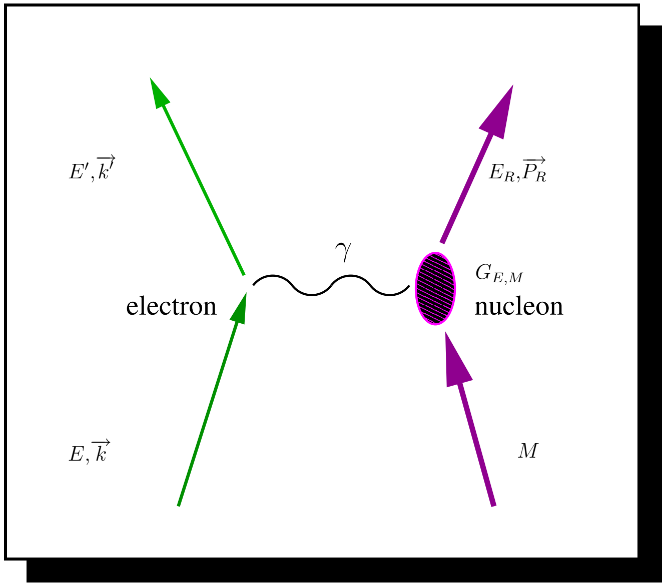


$$F_1^p = 1 \qquad F_1^n = 0$$
$$F_2^p = 1.79 \qquad F_2^n = -1.91$$

In Breit frame $F_1$ and $F_2$ related to charge and spatial curent densities:

$$\rho = J_0 = 2eM[F_1 - \tau F_2]$$
$$J_i = e\bar{u}\gamma_i u[F_1 + F_2]_{i=1,2,3}$$

$$G_E\left(Q^2\right) = F_1(Q^2) - \tau F_2\left(Q^2\right) \qquad G_M\left(Q^2\right) = F_1\left(Q^2\right) + F_2\left(Q^2\right)$$

✳ For a point like probe $G_E$ and $G_M$ are the FT of the charge and magnetizations distributions in the nucleon, with the following normalizations

$Q^2 = 0$ limit: $G_E^p = 1$ $G_E^n = 0$ $G_M^p = 2.79$ $G_M^n = -1.91$

## $G_E^n$ Interpretation

In the NR limit (Breit Frame), $G_E$ is FT of the charge distribution $\rho(r)$:

$$G_E^n\left(\mathbf{q}^2\right) = \frac{1}{(2\pi)^3}\int d^3r\rho(\mathbf{r})e^{(i\mathbf{q}\cdot\mathbf{r})} = 0 - \frac{\mathbf{q}^2}{6}\left\langle r_{ne}^2\right\rangle + \ldots$$

Experimental: Mean square charge radius $\langle r_{ne}^2\rangle$ is negative.

Theory has intuitive explanation:

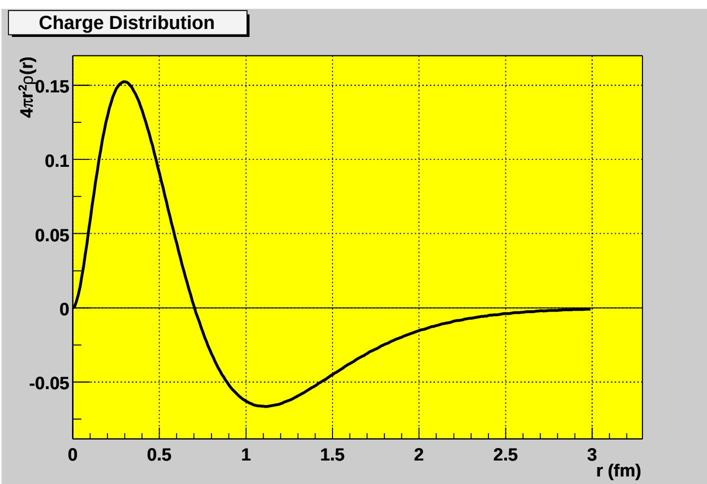


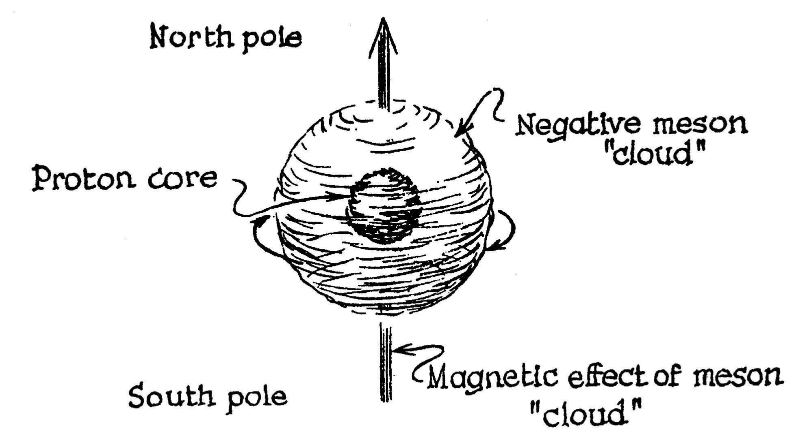


pion-nucleon theory: n = p + $\pi^-$ cloud

valence quark model: n = ddu & spin-spin force $\Rightarrow d \rightarrow$ periphery

# Charge radius, Foldy term

$$\langle r_{ne}^2 \rangle = -6 \frac{dG_E^n(0)}{dQ^2} \quad = \quad -6 \frac{dF_1^n(0)}{dQ^2} + \frac{3}{2M^2} F_2^n(0)$$
$$= \quad \langle r_{\text{in}}^2 \rangle + \langle r_{\text{Foldy}}^2 \rangle$$

Foldy term, $\frac{3\mu_n}{2m_n} = (-0.126)\text{fm}^2$, has nothing to do with the rest frame charge distribution.

$\langle r_{ne}^2 \rangle$ is measured through neutron-electron scattering

$$\langle r_{ne}^2 \rangle = \frac{3m_e a_0}{m_n} b_{ne} = -0.113 \pm 0.003 \pm 0.004\,\text{fm}^2.$$

$\langle r_{\text{in}}^2 \rangle = -0.113 + 0.126 \approx 0$ suggesting that the spatial charge extension seen in $F_1$ is about 0 or very small. Recent Work:

N. Isgur, Phys. Rev. Lett. 83, 272 (1999)

M. Bawin & A.A. Coon, Phys. Rev. C. 60, 025207 (1999)

$G_E^n$ arises from the neutron's rest frame charge distribution.

A. Glozman & D. Riska, Phys. Lett. B 459 (1999) 49.

Pionic loop fluctuations make minute contribution to $\langle r_{\text{in}}^2 \rangle$.

## Why measure $G_E^n$ ?

- ✳ FF are fundamental quantities
- ✳ Test of QCD description of the nucleon

  Symmetric quark model, with all valence quarks with same wf: $G_E^n \equiv 0$

  $G_E^n \neq 0 \rightarrow$ details of the wavefunctions

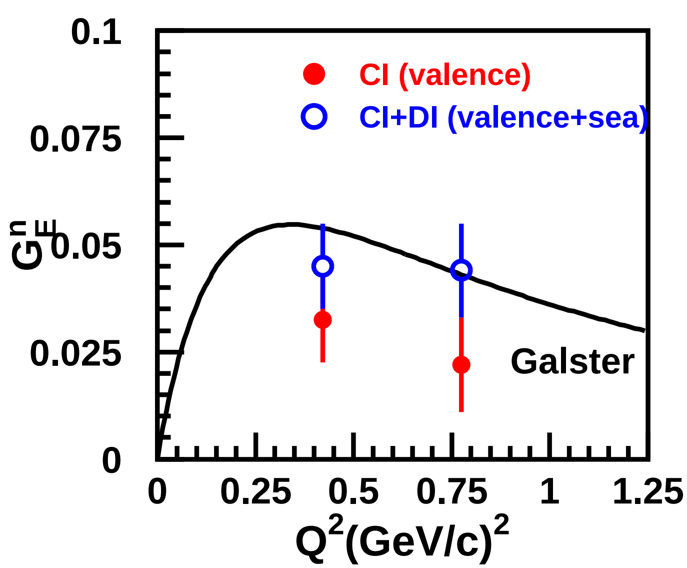


Dong, Liu, Williams, PRD 58 074504

- ✳ Sensitive to sea quark contributions
- ✳ Soliton model: $\rho(r)$ at large $r$ due to sea quarks

## Necessary for study of nuclear structure.

- ✳ Few body structure functions

# Proton Form Factor Data

Rosenbluth separation

$$\frac{d\sigma}{d\Omega} = \frac{\sigma_{Mott}}{(1+\tau)}\frac{E'}{E_0}\left[G_E^2 + \underbrace{\tau(1+(1+\tau)2\tan^2(\theta/2))G_M^2}\right]$$

- ✳ $G_M^p$ well measured via Rosenbluth, but not $G_E^p$ hence Recoil Polarization
- ✳ Dipole Parametrization: Good description of early $G_{E,M}^p$ data

$$G_E^p = \frac{G_M^p}{\mu_p} = G_D = \left(1 + \frac{Q^2}{0.71}\right)^{-2}$$

$G_D = \left(1 + \frac{Q^2}{k^2}\right)^{-2}$ implies an exponential charge distribution: $\rho(r) \propto e^{-kr}$

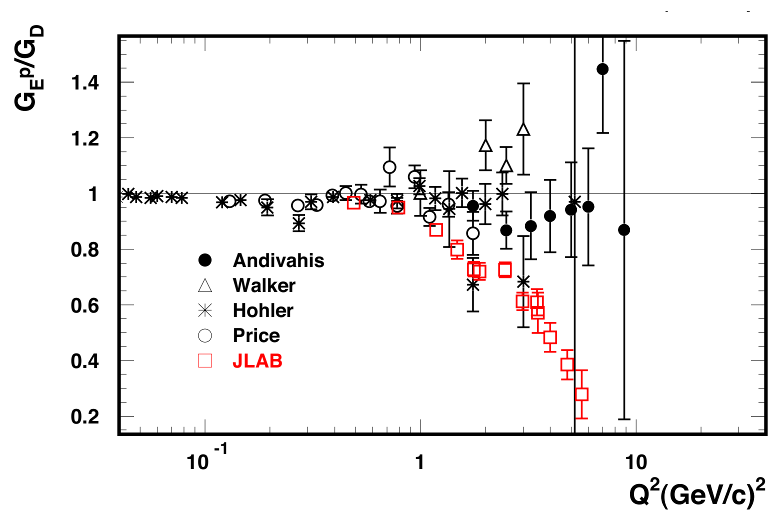


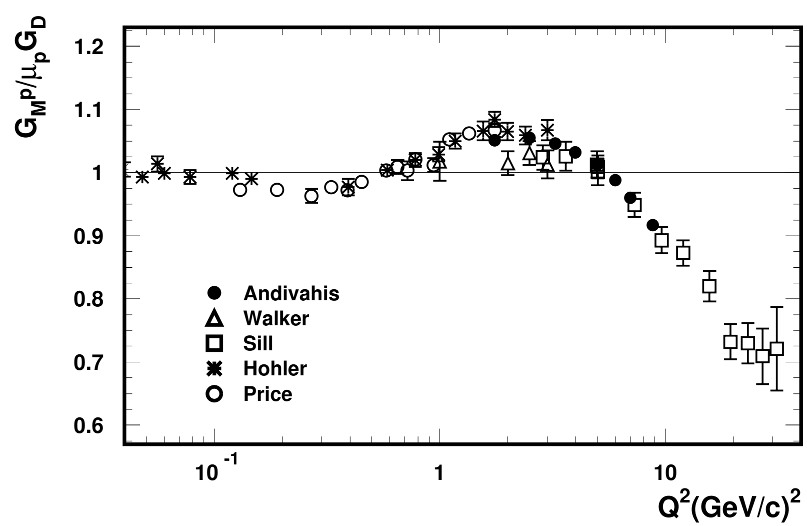

## Neutron Form Factors without Polarization

No neutron target, $G_M^n$ dominates $G_E^n$, proton dominates neutron

Traditional techniques used to measure $G_M^n$ and $G_E^n$ have been:

- ✳ Elastic scattering $^2\mathrm{H}(e, e')^2\mathrm{H}$
- ✳ Inclusive quasielastic scattering: $^2\mathrm{H}(e, e')X$
- ✳ Neutron in coincidence with electron: $^2\mathrm{H}(e, e'n)p$
- ✳ Neutron in anti-coincidence with electron: $^2\mathrm{H}(e, e'\bar{\mathrm{p}})\mathrm{p}$
- ✳ Ratio techniques $\frac{d(e,e'n)p}{d(e,e'p)n}$ minimizes roles of g.s. wavefunction and FSI.

  Quasielastic kinematics and simplest nucleus

# Measurements of the Neutron Form Factors

| Target | Type | $Q^2 (GeV/c)^2$ | Deduced quantities | Reference |
|---|---|---|---|---|
| $^2H$ | elastic | 0.004-0.032 | $G_{En}$ | F.A. Bumiller *et al.*, PRL 25, 1774 (1970) |
| $^2H$ | elastic | 0.012-0.085 | $G_{En}$ | Drickey & Hand, PRL 9, 1774 (1962) |
| $^2H$ | elastic | 0.002-0.16 | $G_{En}$ | G.G. Simon, *et al.*, NP A364, 285 (1981) |
| $^2H$ | ratio | 0.11 | $G_{Mn}$ | H.A. Anklin *et al.*, PL B336, 313 (1994) |
| $^2H$ | quasielastic | 0.11-0.16 | $G_{En}, G_{Mn}$ | B. Grossette *et al.*, PR 141, 1435 (1966) |
| $^2H$ | elastic | 0.116-0.195 | $G_{En}, G_{Mn}$ | P. Benaksas *et al.*, PRL 13, 1774 (1964) |
| $^2H$ | coincidence | 0.109-0.255 | $G_{Mn}$ | P. Markowitz *et al.* PR C48, R5 (1993) |
| $^2H$ | quasielastic | 0.06-0.3 | $G_{En}, G_{Mn}$ | E.B. Hughes *et al.* PR 146, 973 (1966) |
| $^2H$ | elastic | 0.116-0.195 | $G_{Mn}$ | J.I. Friedman *et al.* PR 120, 992 (1960) |
| $^2H$ | elastic | 0.2-0.56 | $G_{En}$ | S. Galster *et al.* NP B32, 221 (1971) |
| $^2H$ | ratio | 0.22-0.58 | $G_{En}, G_{Mn}$ | P. Stein *et al.* PRl 16, 592 (1966) |
| $^2H$ | ratio | 0.125-0.605 | $G_{Mn}$ | E.E. Bruins *et al.* PRL 75, 21 (1995) |
| $^2H$ | ratio | 0.2-0.9 | $G_{Mn}$ | H.A. Anklin *et al.*, PL B428, 248 (1998) |
| | | 0.2-0.9 | $G_{Mn}$ | G. Kubon *et al.*, PL B524, 26 (2002) |
| $^2H$ | elastic | 0.04-0.72 | $G_{En}$ | S. Platchov *et al.* NP A510, 740 (1990) |
| $^2H$ | ratio | 0.39-0.78 | $G_{En}, G_{Mn}$ | W. Bartel *et al.* PL 30B, 285 (1969) |
| $^2H$ | quasielastic | 0.48-0.83 | $G_{Mn}$ | A.S. Esaulov *et al.* Sov. J. NP 45, 258 (1987) |
| $^2H$ | quasielastic | 0.04-1.2 | $G_{En}, G_{Mn}$ | E.B. Hughes *et al.* PR 139, B458 (1965) |
| $^2H$ | quasielastic | 0.04-0.2 | $G_{Mn}$ | D. Braess *et al.* Zeit Phys. 198, 527 (1967)reanalysis of Hughes |
| $^2H$ | quasielastic | 0.39-1.5 | $G_{En}, G_{Mn}$ | W. Bartel *et al.* NP B58, 429 (1973) |
| $^2H$ | ratio | 1.0-1.53 | $G_{En}, G_{Mn}$ | W. Bartel *et al.* PL 39B, 407(1972) |
| $^2H$ | anticoincidence | 0.28-1.8 | $G_{En}, G_{Mn}$ | K.M. Hanson *et al.* PR D8, 753 (1973) |
| $^2H$ | quasielastic | 0.75-2.57 | $G_{Mn}$ | R.G. Arnold *et al.* PRL 61, 806 (1988) |
| $^2H$ | quasielastic | 1.75-4.0 | $G_{En}, G_{Mn}$ | A. Lung *et al.* PRL 70, 718 (1993) |
| $^2H$ | anticoincidence | 0.27-4.47 | $G_{En}, G_{Mn}$ | R.J. Budnitz *et al.* PR 173, 1357 (1968) |
| $^2H$ | quasielastic | 2.5-10.0 | $G_{Mn}$ | S. Rock *et al.* PRL 49, 1139 (1982) |

$G_M^n$ unpolarized

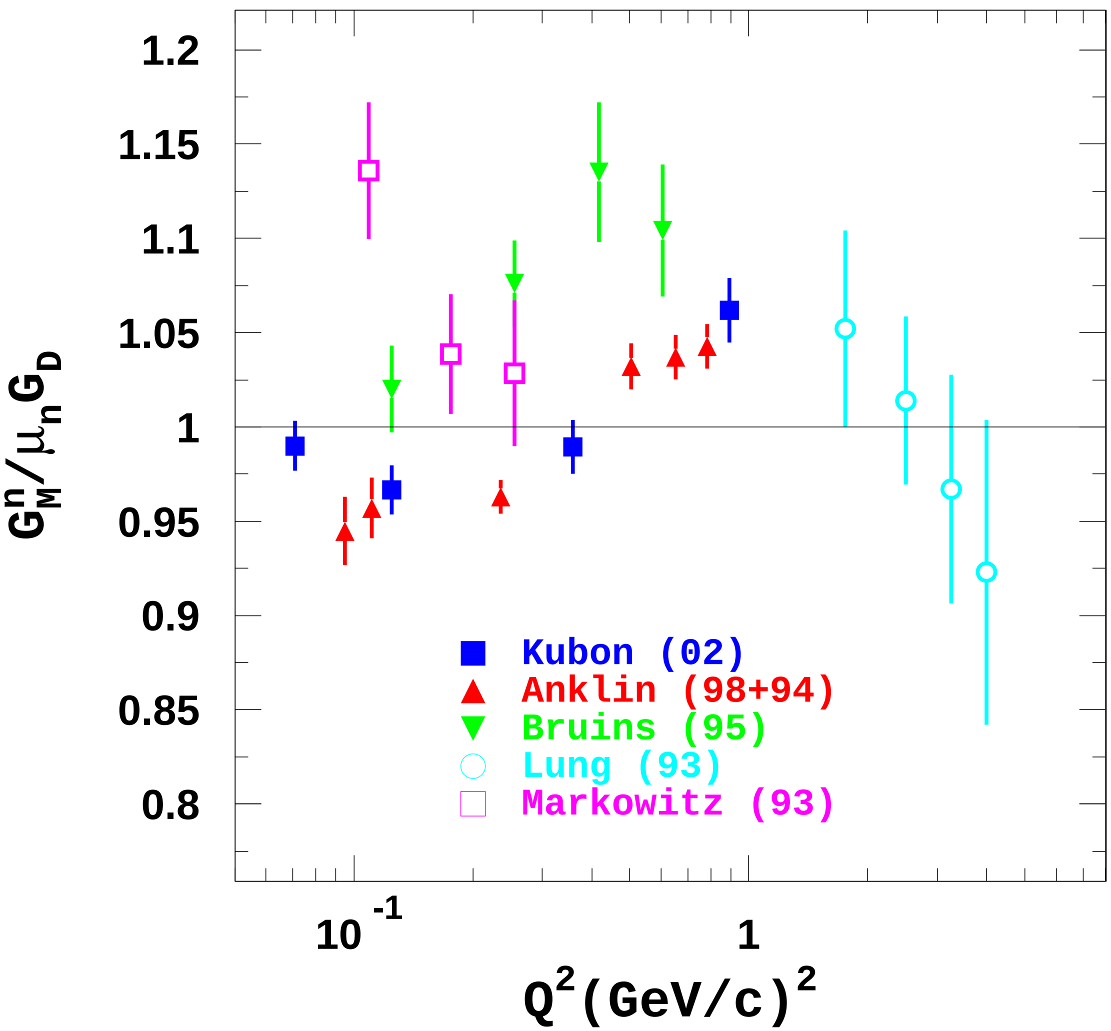


| | |
|---|---|
| Kubon | ratio |
| Anklin | ratio |
| Bruins | ratio |
| Lung | $D(e,e')X$ |
| Markowitz | $D(e,e'n)p$ |

$$\text{ratio} \equiv \frac{D(e,e'n)p}{D(e,e'p)n}$$

## $G_M^n$ unpolarized and polarized

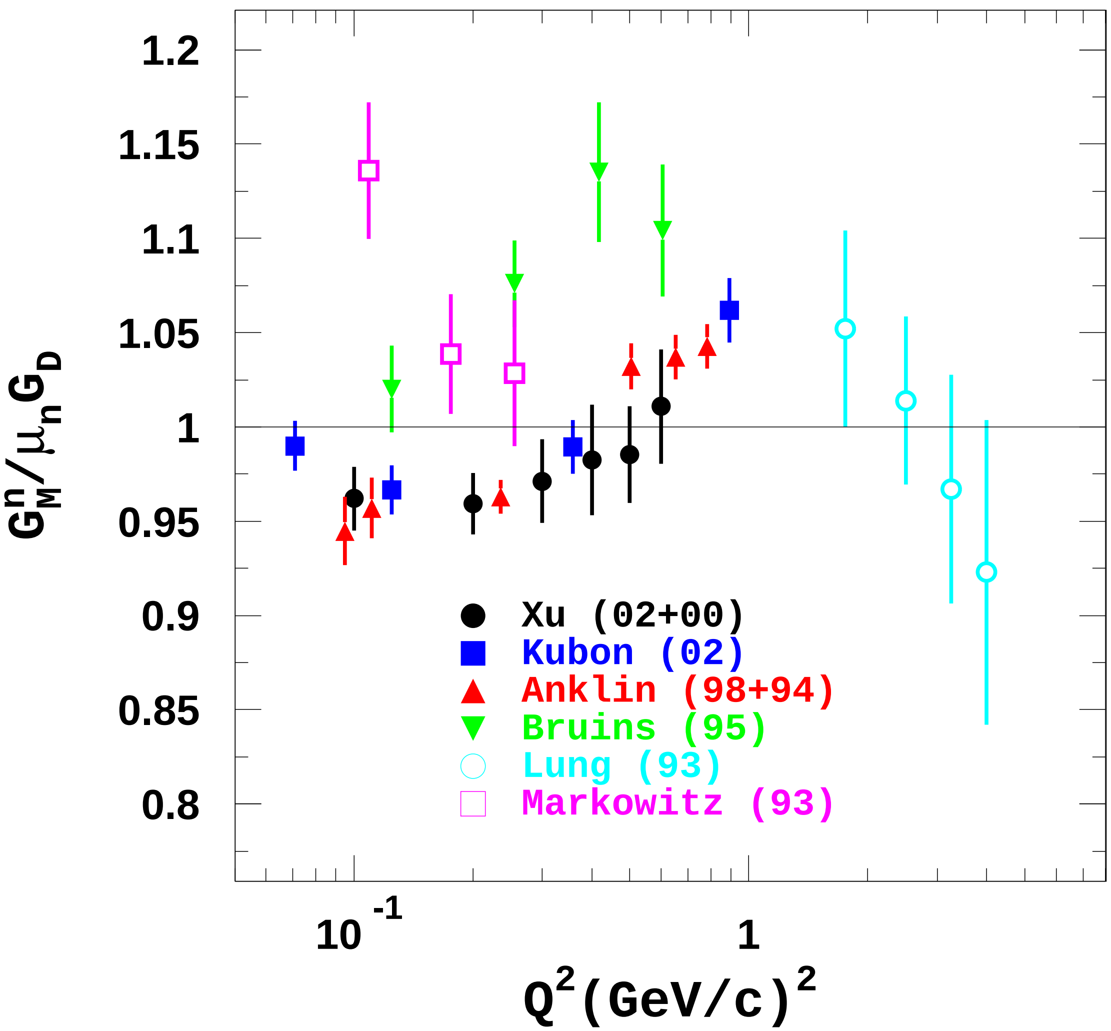


| | |
|---|---|
| Kubon | ratio |
| Anklin | ratio |
| Bruins | ratio |
| Lung | $D(e,e')X$ |
| Markowitz | $D(e,e'n)p$ |
| Xu | $\overrightarrow{^3\text{He}}(\vec{e},e')X$ |

$$\text{ratio} \equiv \frac{D(e,e'n)p}{D(e,e'p)n}$$

# $G_E^n$ Before Polarization

No free neutron – extract from $e - D$ elastic scattering:

$$\frac{d\sigma}{d\Omega} = \sigma_{NS}\left[A\left(Q^2\right) + B\left(Q^2\right)\tan^2\left(\frac{\theta_e}{2}\right)\right]$$

small $\theta_e$ approximation

$$\frac{d\sigma}{d\Omega} = \cdots (G_E^p + G_E^n)^2 \overbrace{\int \left[u(r)^2 + w(r)^2\right] j_0(\frac{qr}{2})dr}^{C_E(q)} \cdots$$

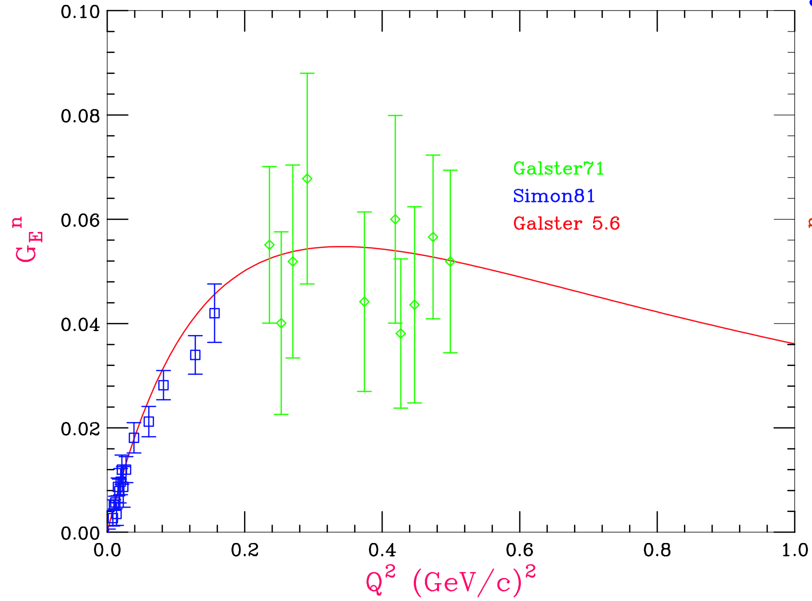


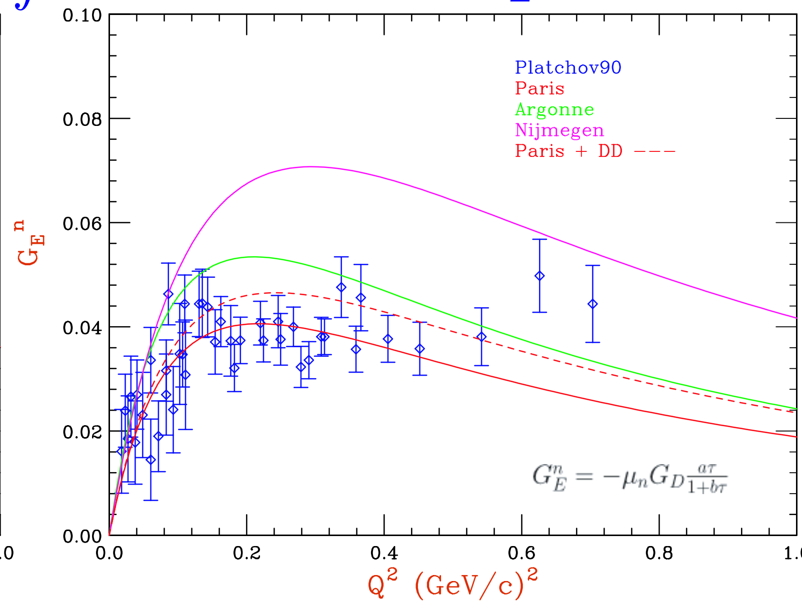


Galster Parametrization: $G_E^n = -\frac{\tau\mu_n}{1+5.6\tau} G_D$

## $G_E^n$ from Elastic Scattering – $\mathrm{D}(e, e'\vec{\mathrm{d}})$

Components of the tensor polarization give useful combinations of the form factors,

$$t_{20} = \frac{1}{\sqrt{2}S}\left\{\frac{8}{3}\tau_d G_C G_Q + \frac{8}{9}\tau_d^2 G_Q^2 + \frac{1}{3}\tau_d\left[1 + 2(1+\tau_d)\tan^2(\theta/2)\right] G_M^2\right\}$$

$G_Q(Q^2) = (G_E^p + G_E^n)C_Q(q)$ suffers less from theoretical uncertainties than $A(Q^2)$.

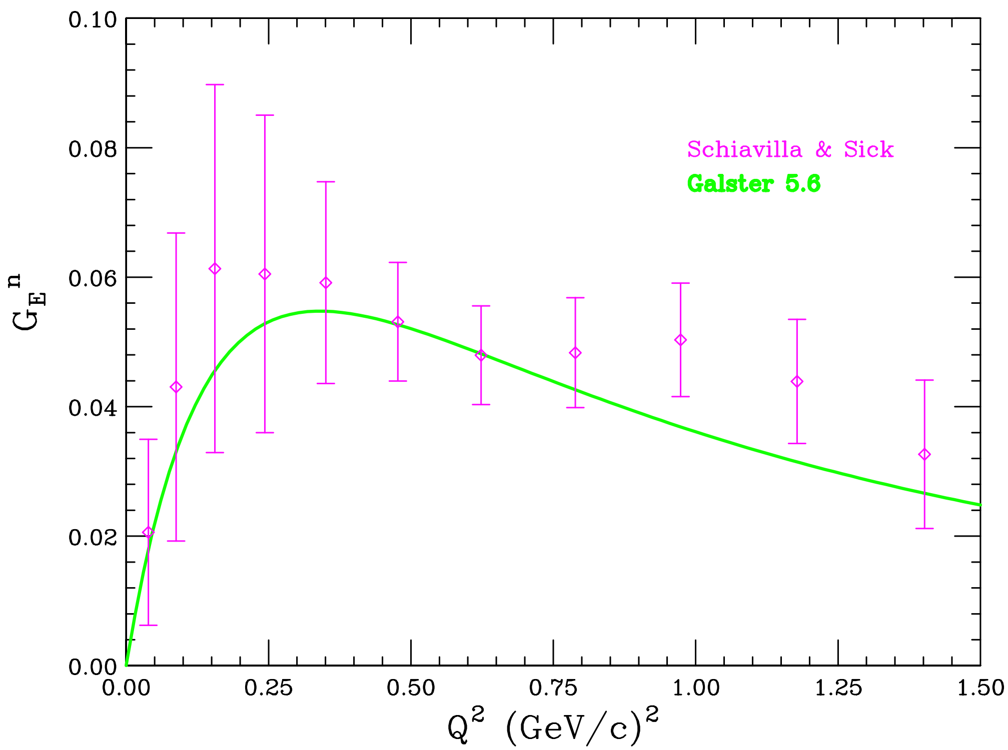


$G_E^n$ can be extracted to larger momentum transfers.

# $G_E^n$ at large $Q^2$ through ${}^2\mathrm{H}(e, e')X$

PWIA model $\sigma$ is incoherent sum of p and n cross section folded with deuteron structure.

$$\sigma = (\sigma_p + \sigma_n) I(u, w)$$
$$= \varepsilon R_L + R_T$$

✷ Extraction of $G_E^n$:

Rosenbluth Separation $\Rightarrow R_L$

Subtraction of proton contribution

✷ Problems:

Unfavorable error propagation

Sensitivity to deuteron structure

SLAC: *A. Lung et al, PRL. 70, 718 (1993)*

$\rightarrow$No indication of non-zero $G_E^n$

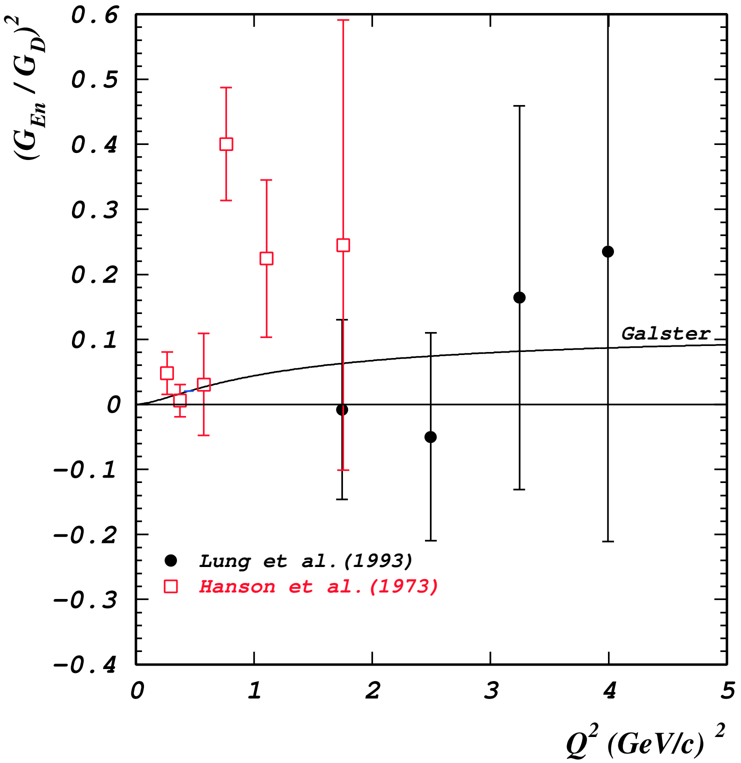


If $G_E^n$ is small at large $Q^2$ then $F_1^n$ must cancel $\tau F_2^n$, begging the question, how does $F_1^n$ evolve from 0 at $Q^2 = 0$ to cancel $\tau F_2^n$ at large $Q^2$?

## Models of Nucleon Form Factors

| | |
|---|---|
| VMD | $F(Q^2) = \sum_i \frac{C_{\gamma V_i}}{Q^2+M^2_{V_i}} F_{V_i N}(Q^2)$ |
| | breaks down at large $Q^2$ |
| CBM | Lu, Thomas, Williams (1998) |
| pQCD | $F_2 \propto F_1 \left(\frac{M}{Q^2}\right)$ helicity conservation |
| | Counting rules: $F_1 \propto \frac{\alpha_s^2(Q^2)}{Q^4}$ |
| | $Q^2 F_2/F_1 \rightarrow$ constant |
| | JLAB proton data: $QF_2/F_1 \rightarrow$ constant |
| Hybrid VMD-pQCD | GK, Lomon |
| Lattice | Dong .. (1998) |
| RCQM | point form (Wagenbrunn..) |
| | light front (Cardarelli ..) |
| Soliton | Holzwarth |
| LFCBM | Miller |
| Helicity non-conservation | pQCD (Ralston..) LF (Miller..) |

# Theoretical Models

## Vector Meson Dominance

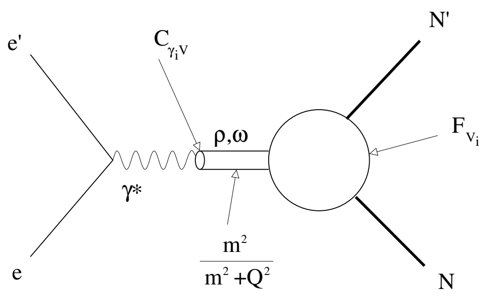


Interaction in terms of coupling strengths of virtual photon and vector mesons and vector mesons and nucleon. Success at low and moderate $Q^2$ offset by failure to accomodate pQCD.

## pQCD

High $Q^2$ helicity conservation requires that $Q^2F_1/F_2 \longrightarrow$ constant as $F_2$ helicity flip arises from second order corrections and are suppressed by an additional factor of $1/Q^2$. Furthermore for $Q^2 \gg \Lambda_{QCD}$ counting rules find $F_1 \propto \alpha_s(Q^2)^2/Q^4$. Thus $F_1 \propto \frac{1}{Q^4}$ and $F_2 \propto \frac{1}{Q^6} \Rightarrow Q^2\frac{F_2}{F_1} \longrightarrow$ constant.

## Lattice calculations of form form factors

Fundamental but limited in stat. accuracy
Dong *et al* PRD58, 074504 (1998)

## QCD based Models

Try to capture aspects of QCD
RCQM, Di-quark model, CBM

## Hybrid Models

Failure to follow the high $Q^2$ behavior suggested by pQCD led GK to incorporate pQCD at high $Q^2$ with the low VMD behavior. Inclusion of $\phi$ by GK had significant effect on $G_E^n$. Lomon has updated with new fits to selected data.

Helicity non-conservation shows up in the light front dynamics analysis of Miller which predicted $Q\frac{F_2}{F_1} \longrightarrow$ constant and the violation of helicity conservation. Ralston's pQCD model also predicts that $Q\frac{F_2}{F_1} \longrightarrow$ constant. Both models include quark orbital angular momentum.

# Theoretical Models

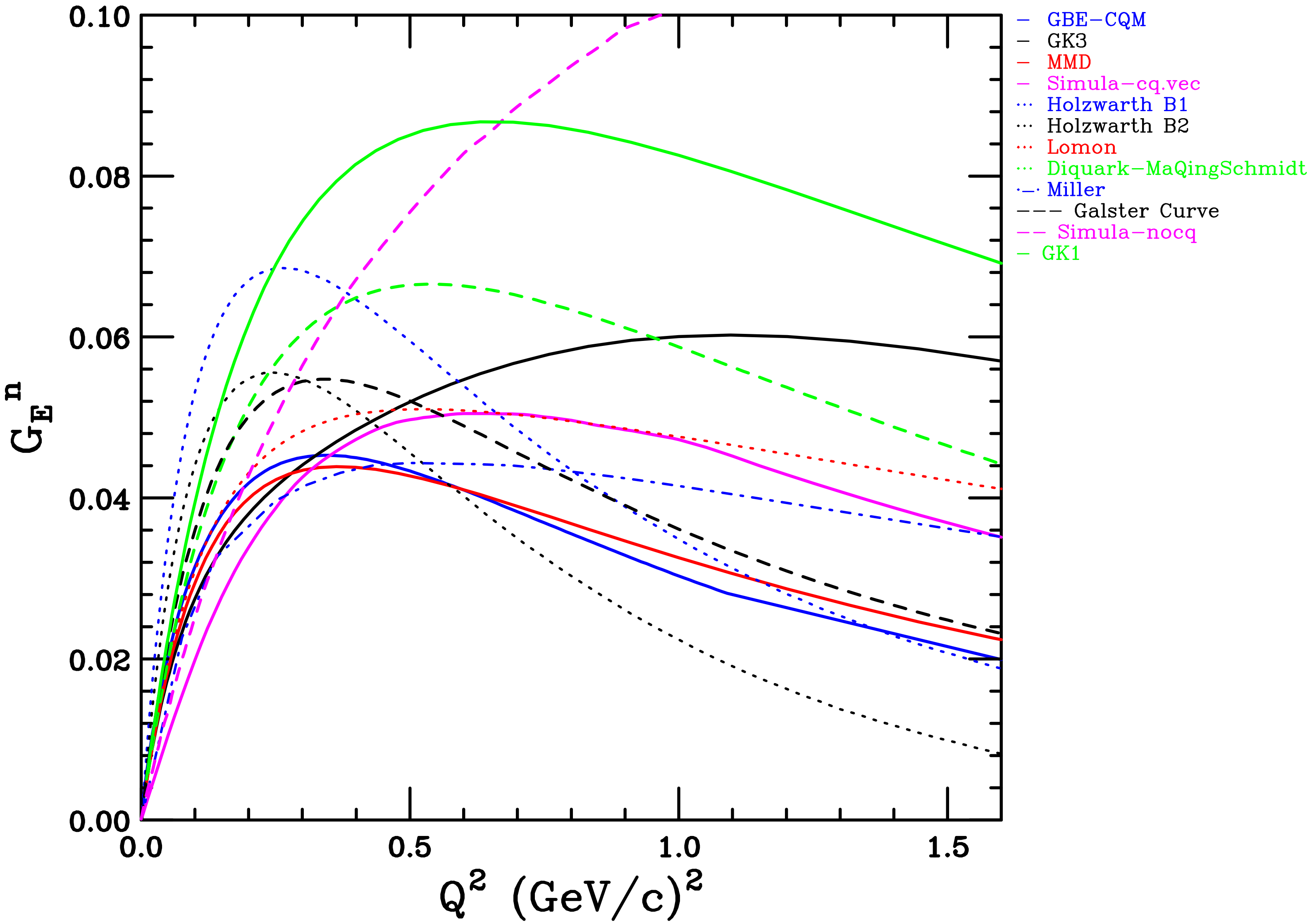

## Spin Correlations in elastic scattering

- ∗ Dombey, Rev. Mod. Phys. **41** 236 (1968): $\vec{p}(\vec{e}, e')$
- ∗ Akheizer and Rekalo, Sov. Phys. Doklady **13** 572 (1968): $p(\vec{e}, e', \vec{p})$
- ∗ Arnold, Carlson and Gross, Phys. Rev. C **23** 363 (1981): $^2\mathrm{H}(\vec{e}, e'\vec{n})p$

## Essential statement

Exploit spin degrees of freedom

- ∗ $\mathcal{O} \propto G_E \times G_M$ instead of $\mathcal{O} \propto G_E^2 + G_M^2$

### Early work at Bates, Mainz

- ∗ $^2\mathrm{H}(\vec{e}, e'\vec{n})p$ , Eden *et al.* (1994)
- ∗ $^1\mathrm{H}(\vec{e}, e'\vec{p})$ , Milbrath *et al.* (1998)
- ∗ $^3\overrightarrow{\mathrm{He}}(e, e')$, Woodward, Jones, Thompson, Gao (1990 - 1994)
- ∗ $^3\overrightarrow{\mathrm{He}}(e, e'n)$, Meyerhoff, (1994)

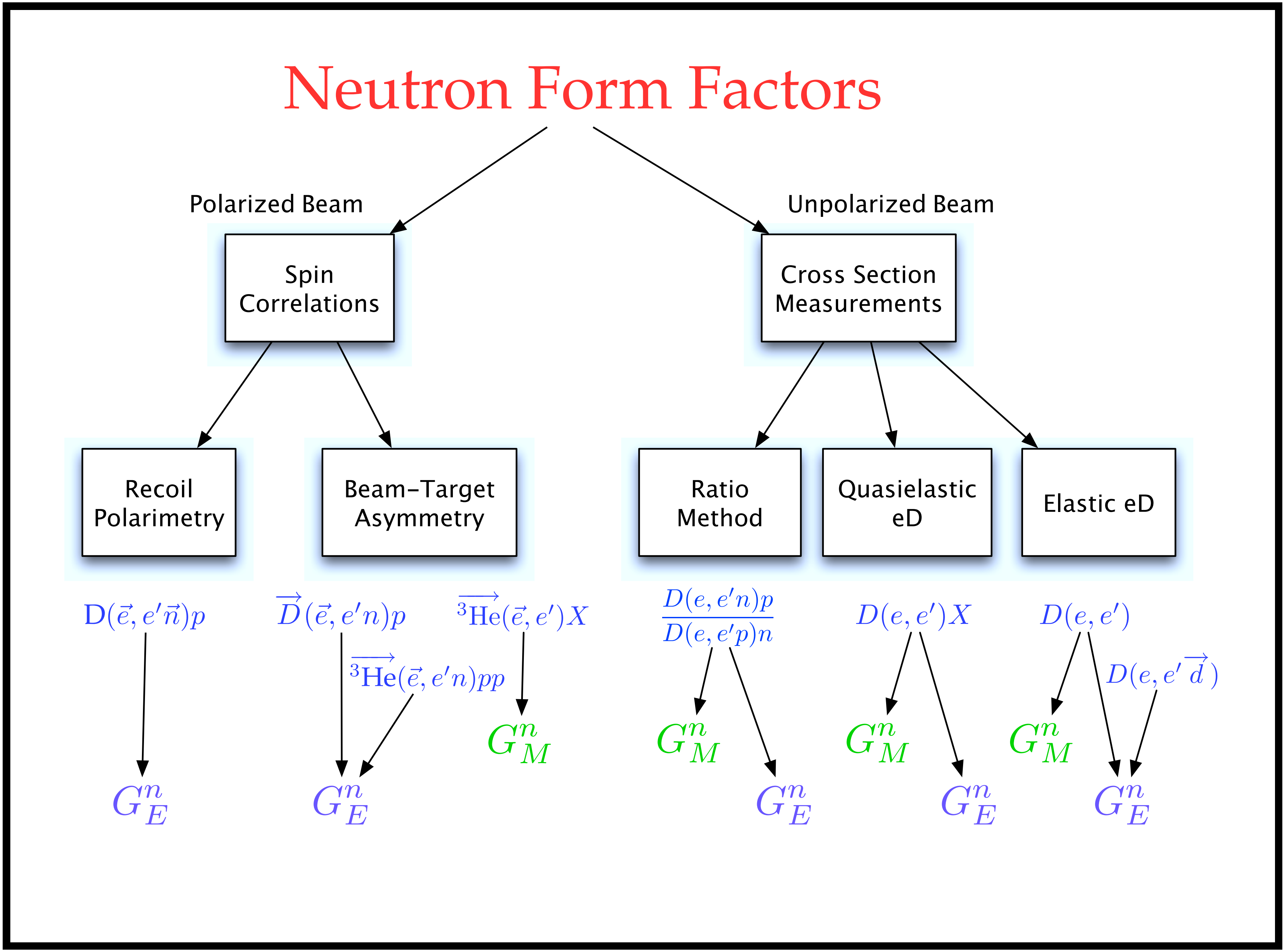
Neutron Form Factors
Polarized Beam
Unpolarized Beam
Spin Correlations
Cross Section Measurements
Recoil Polarimetry
Beam−Target Asymmetry
Ratio Method
Quasielastic eD
Elastic eD
$\mathrm{D}(\vec{e}, e'\vec{n})p$
$\vec{D}(\vec{e}, e'n)p$
$\overrightarrow{{}^3\mathrm{He}}(\vec{e}, e')X$
$\overrightarrow{{}^3\mathrm{He}}(\vec{e}, e'n)pp$
$\frac{D(e,e'n)p}{D(e,e'p)n}$
$D(e,e')X$
$D(e,e')$
$D(e,e'\vec{d})$
$G_E^n$
$G_E^n$
$G_M^n$
$G_M^n$
$G_E^n$
$G_M^n$
$G_E^n$
$G_M^n$
$G_E^n$

## $G_E^n$ from spin observables

No free neutron targets – scattering from $^2$H or $^3$He– can not avoid engaging the details of the nuclear physics.

Minimize sensitivity to the how the reaction is treated and maximize the sensitivity to the neutron form factors by working in quasifree kinematics. Detect neutron.

- ✳ Indirect measurements: The experimental asymmetries ($\xi_{s'}$, $A_V^{ed}$, $A_{\text{exp}}^{qe}$) are compared to theoretical calculations.
- ✳ Theoretical calculations are generated for scaled values of the form factor.
- ✳ Form factor is extracted by comparison of the experimental asymmetry to acceptance averaged theory. Monte Carlo
- ✳ Polarized targets

  The deuteron and $^3$He only approximate a polarized neutron

  Scattering from other unpolarized materials, $f$ dilution factor

# Recoil Polarization

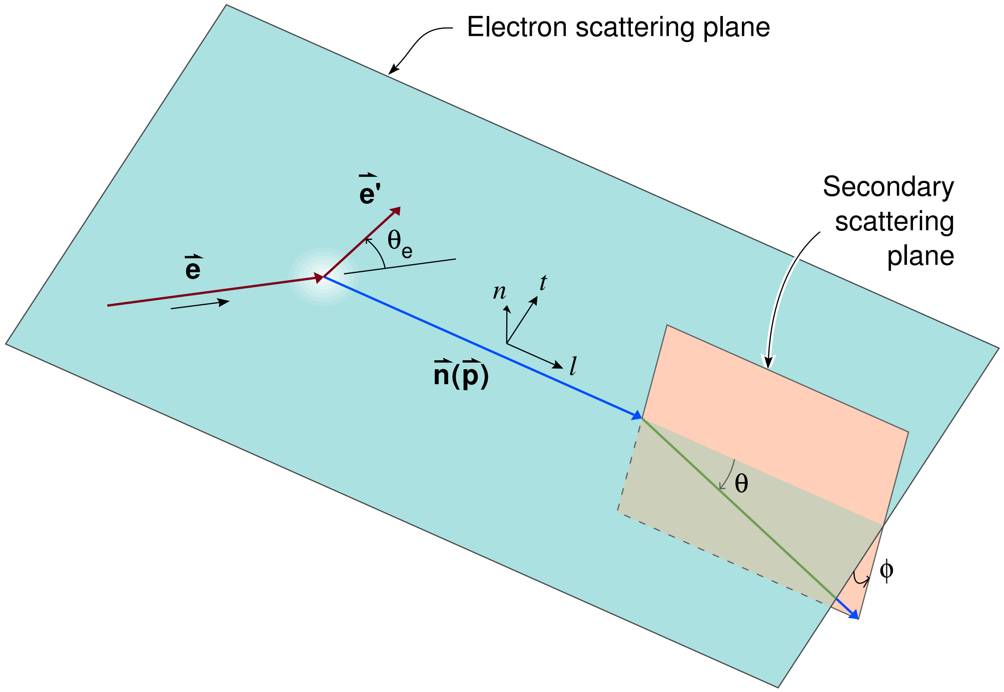


$$I_0 P_t = -2\sqrt{\tau(1+\tau)}\,G_E G_M \tan(\theta_e/2)$$
$$I_0 P_l = \frac{1}{M_N}(E_e + E_{e'})\sqrt{\tau(1+\tau)}\,G_M^2 \tan^2(\theta_e/2)$$

$$\frac{G_E}{G_M} = -\frac{P_t}{P_l}\frac{(E_e+E_{e'})}{2M_N}\tan\left(\frac{\theta_e}{2}\right)$$

Direct measurement of form factor ratio by measuring the ratio of the transfered polarization $P_t$ and $P_l$

## Recoil Polarization – Principle and Practice

- ✳ Interested in transfered polarization, $P_l$ and $P_t$, at the target
- ✳ Polarimeters are sensitive to the perpendicular components only, $P_n^{\rm pol}$ and $P_t^{\rm pol}$

  Measuring the ratio $P_t/P_l$ requires the precession of $P_l$ by angle $\chi$ before the polarimeter.

- ✳ If polarization precesses $\chi$ (e.g. in a dipole with $\vec{B}$ normal to scattering plane):

  $P_t^{\rm pol} = \sin\chi \cdot P_l + \cos\chi \cdot P_t$

  For $\chi = 90^o$, $P_t^{\rm pol} = P_l$ and is related to $G_M^2$

  For $\chi = 0^o$, $P_t^{\rm pol} = P_t$ and is related to $G_E G_M$

- ✳ $G_E^n/G_M^n$ via ${}^2{\rm H}(\vec{e}, e'\vec{n})p$ in JLAB's Hall C - Charybdis and N-Pol

Quality of polarimeter data optimized by taking advantage of proper flips (helicity reversals).

$$L_1 = N_o[1 + pA_y(\theta + \alpha)]$$

$$R_2 = N_o[1 - pA_y(\theta + \beta)]$$

$$R_1 = N_o[1 - pA_y(\theta + \alpha)]$$

$$L_2 = N_o[1 + pA_y(\theta + \beta)]$$

Using the geometric means, $L \equiv \sqrt{L_1 L_2}$ and $R \equiv \sqrt{R_1 R_2}$, the false (instrumental) asymmetries, $\alpha$ and $\beta$, cancel.

$$\xi = pA_y = \frac{L - R}{L + R}$$

## $G_E^n$ in Hall C, E93-038

Recoil polarization, $^2\mathrm{H}(\vec{e}, e'\vec{n})p$

- ✳ In quasifree kinematics, $P_{s'}$ is sensitive to $G_E^n$ and insensitive to nuclear physics
- ✳ Up–down asymmetry $\xi \Rightarrow$ transverse (sideways) polarization $P_{s'} = \xi_{s'}/P_e A_{\mathrm{pol}}$. Requires knowledge of $P_e$ and $A_{\mathrm{pol}}$
- ✳ Rotate the polarization vector in the scattering plane (with Charybdis) and measure the longitudinal polarization, $P_{l'} = \xi_{l'}/P_e A_{\mathrm{pol}}$
- ✳ Take ratio, $\frac{P_{s'}}{P_{l'}}$. $P_e$ and $A_{\mathrm{pol}}$ cancel
- ✳ Three momentum transfers, $Q^2 = 0.45, 1.13$, and $1.45(\mathrm{GeV/c})^2$.
- ✳ Data taking 2000/2001.

# $G_E^n$ in Hall C via $^2\mathrm{H}(\vec{e}, e'\vec{n})p$

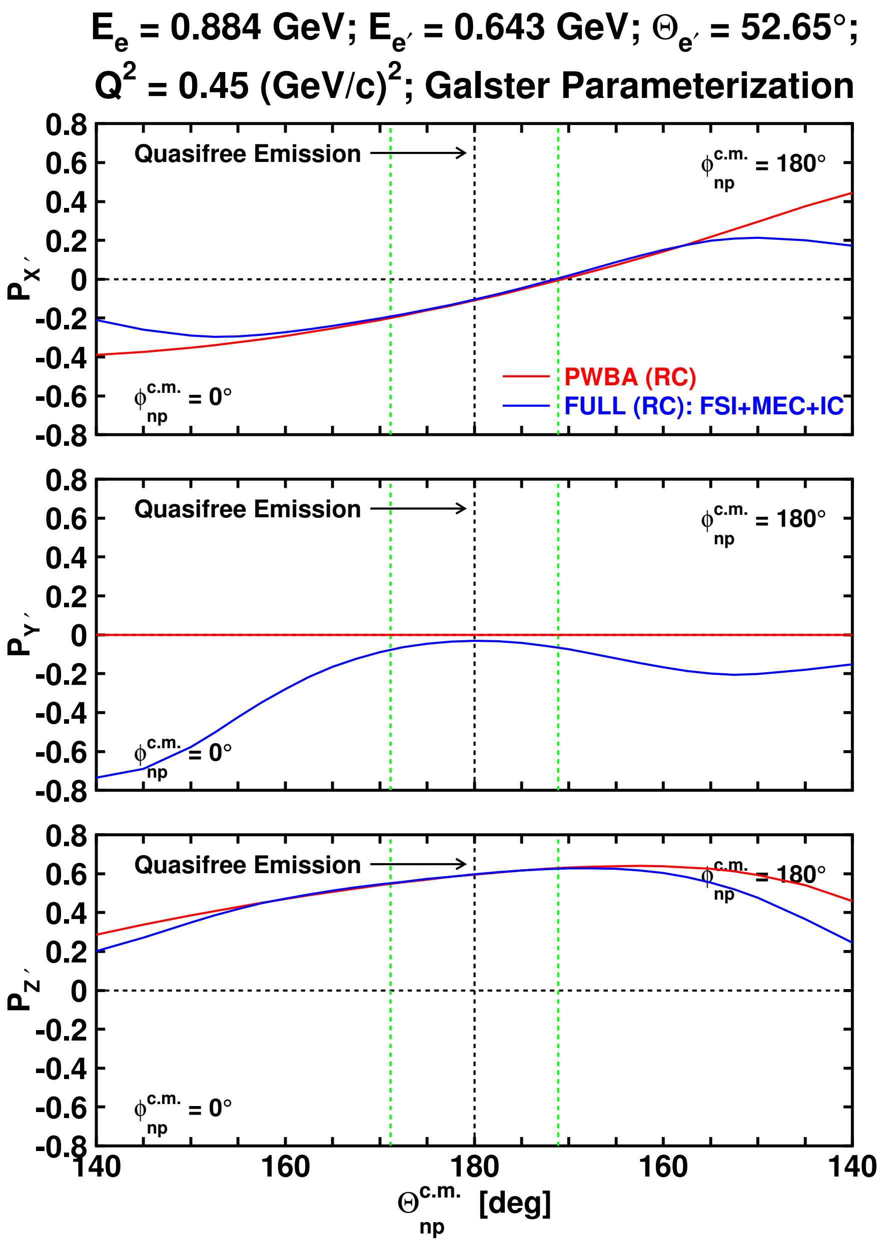

## $G_E^n$ in Hall C via ${}^2\mathrm{H}(\vec{e}, e'\vec{n})p$

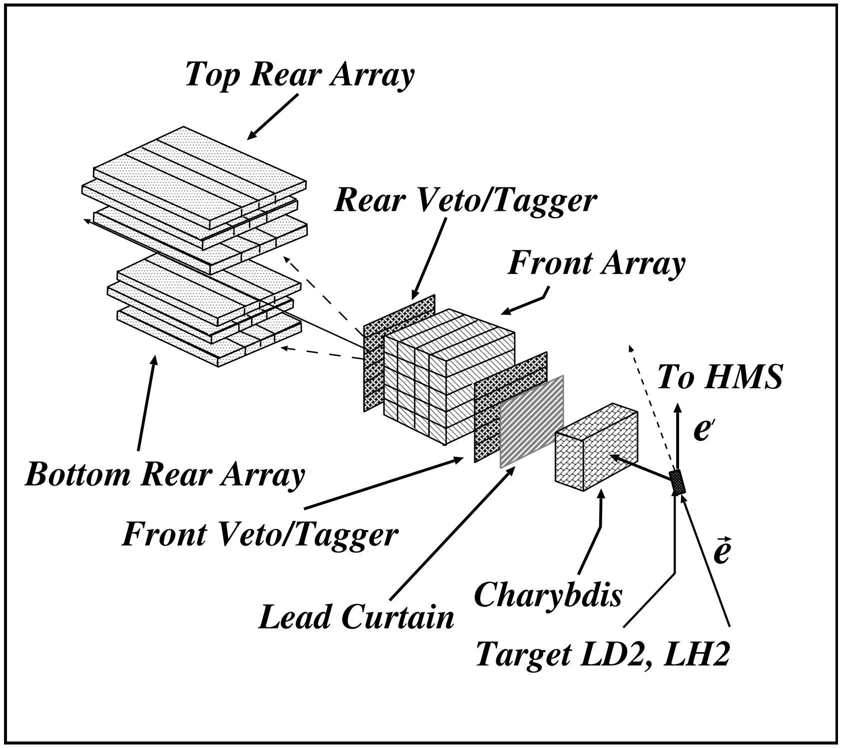


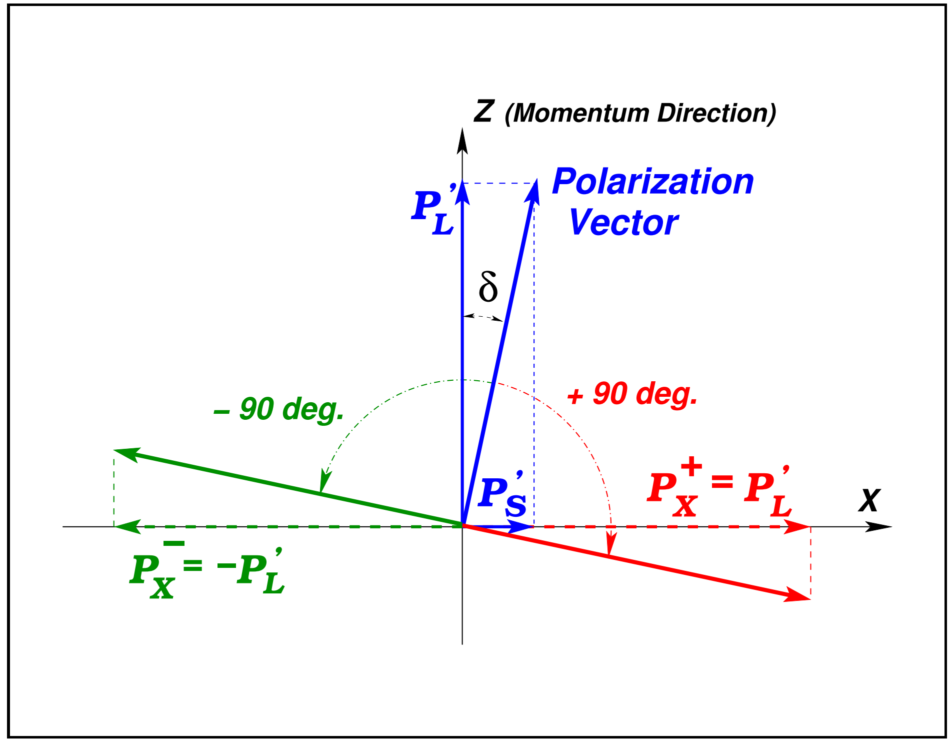


Taking the ratio eliminates the dependence on the analyzing power and the beam polarization → greatly reduced systematics

$$\frac{G_E^n}{G_M^n} = K \tan\delta \qquad \text{where} \qquad \tan\delta = \frac{P_{s'}}{P_{l'}} = \frac{\xi_{s'}}{\xi_{l'}}$$

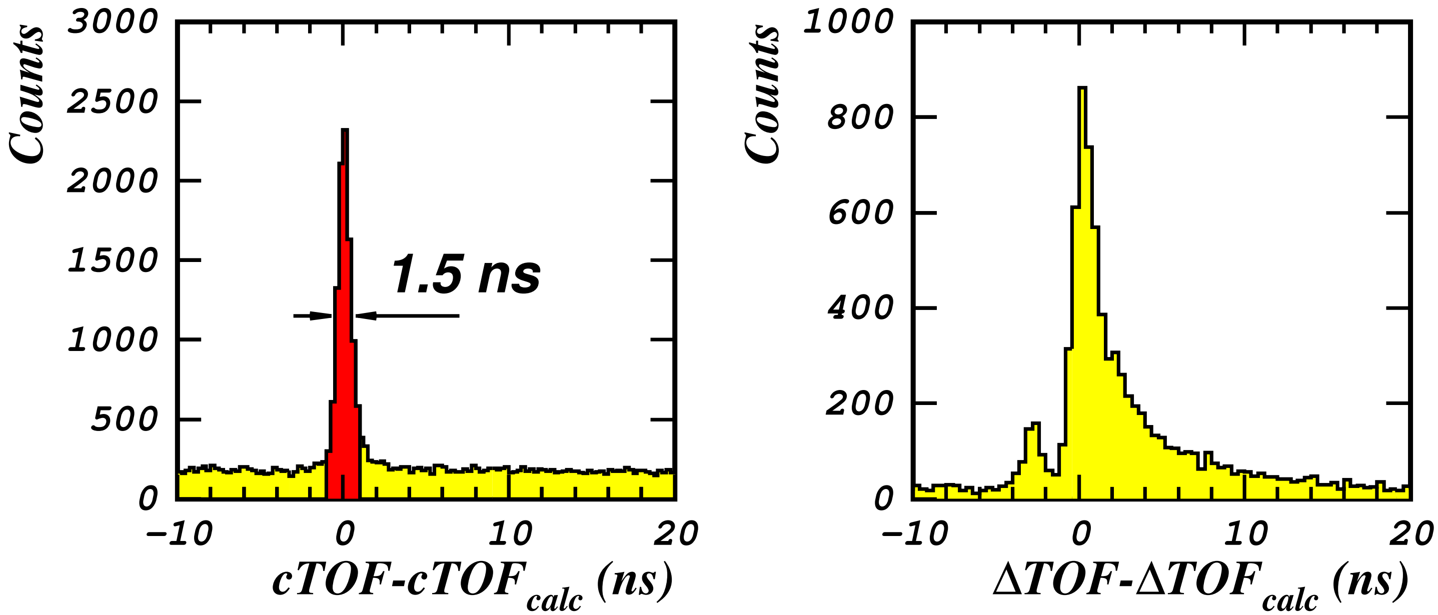


Left: Coincidence TOF for neutrons. Difference between measured TOF and calculated TOF assuming quasi-elastic neutron. Right: $\Delta TOF$ for neutron in front array and neutron in rear array.

$\Delta TOF$ is kept as the four combinations of (-,+) helicity, and (Upper,Lower) detector and cross ratios formed. False asymmetries cancel.

$$r = \left( \frac{N_U^+ N_D^-}{N_U^- N_D^+} \right)^{1/2} \qquad \xi = (r-1)/(r+1)$$

# $G_E^n$ in Hall C via $^2\text{H}(\vec{e}, e'\vec{n})p$

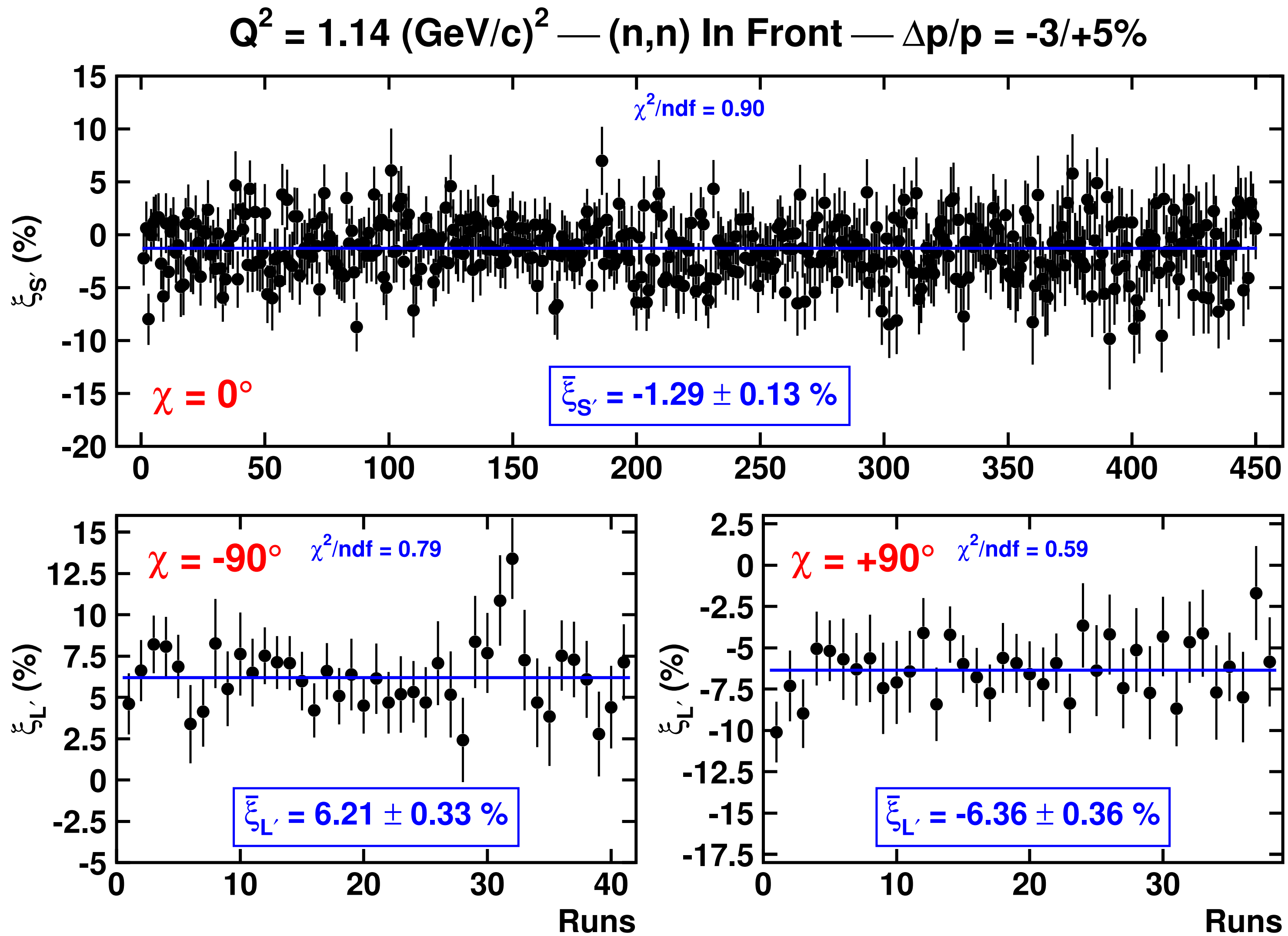

## $G_E^n$ in Hall C via $^2\mathrm{H}(\vec{e}, e'\vec{n})p$

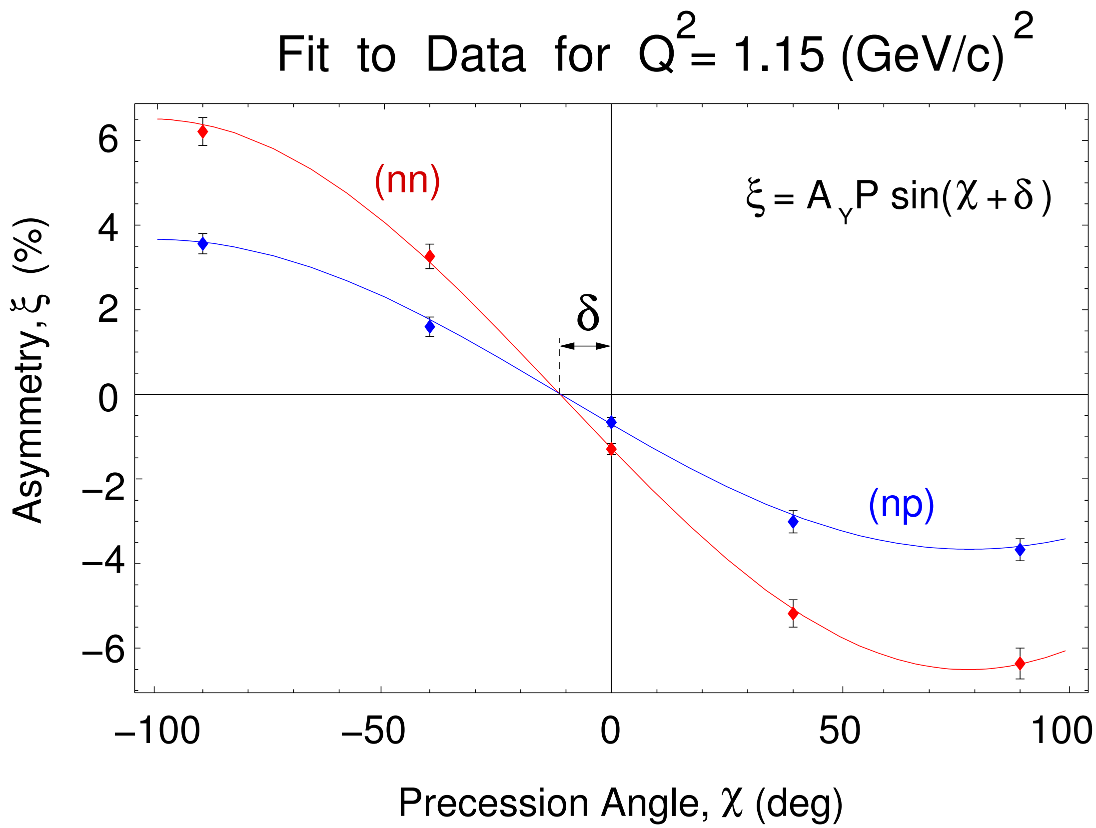

# Results through $^2\mathrm{H}(\vec{e}, e'\vec{n})p$

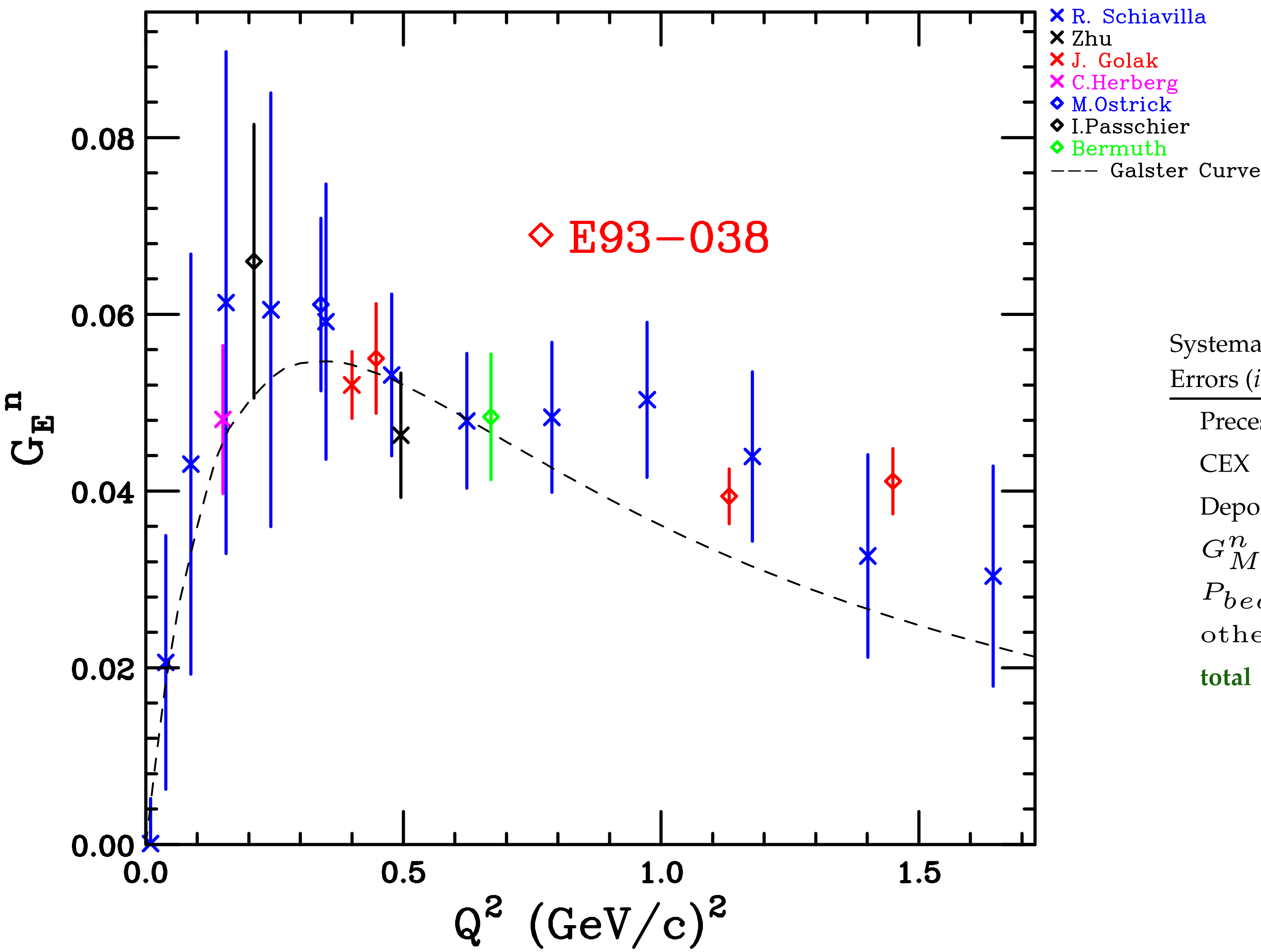


| Systematic Errors (*included*): | |
|---|---|
| Precession $\theta$ | 1% |
| CEX | $<$ 0.2% |
| Depolarization | $\simeq$ 0.5% |
| $G_M^n$ | 2.0% |
| $P_{beam}$ | 1-2% |
| other | 2% |
| **total** | **3%** |

# Beam–Target Asymmetry - Principle

Polarized Cross Section:

$\sigma = \Sigma + h\Delta$

Beam Helicity $h \pm 1$

$$A = \frac{\sigma_+ - \sigma_-}{\sigma_+ + \sigma_-} = \frac{\Delta}{\Sigma}$$

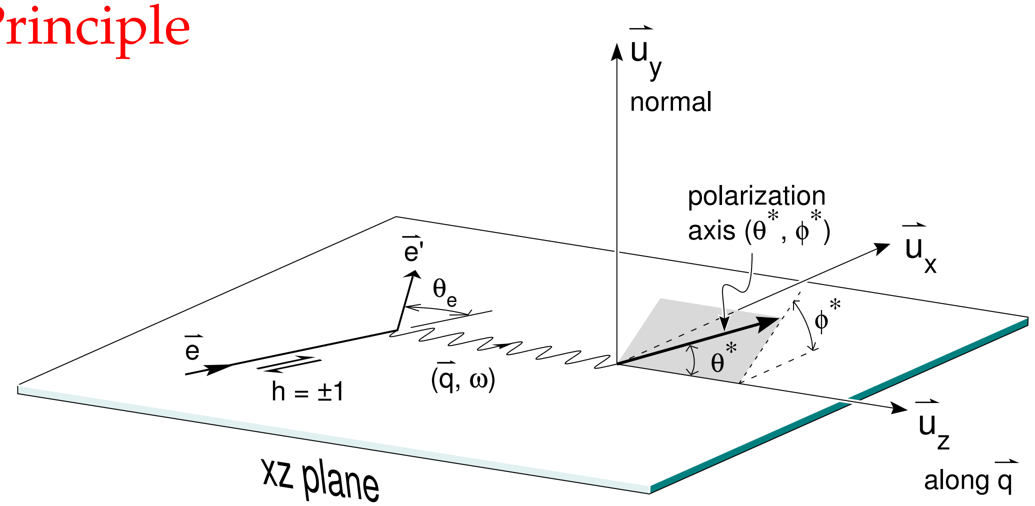


$$A = \frac{\overbrace{a\cos\Theta^\star (G_M)^2}^{A_T} + \overbrace{b\sin\Theta^\star\cos\Phi^\star G_E G_M}^{A_{TL}}}{c\,(G_M)^2 + d\,(G_E)^2}; \quad \varepsilon = \frac{N^\uparrow - N^\downarrow}{N^\uparrow + N^\downarrow} = P_B \cdot P_T \cdot A$$

$\Theta^\star = 90^\circ \quad \Phi^\star = 0^\circ$

$$\Longrightarrow A = \frac{bG_E G_M}{c\,(G_M)^2 + d\,(G_E)^2}$$

$\Theta^\star = 0^\circ \quad \Phi^\star = 0^\circ$

$$\Longrightarrow A = \frac{aG_M^2}{c\,(G_M)^2 + d\,(G_E)^2}$$

## Experimental Asymmetry

### Quasi-Elastic Scattering off Polarized Deuteron

$$\epsilon = P_e \frac{(1-\beta)A_e + (1+\alpha\beta)P_t^V A_{ed}^V + (1-\beta\gamma)P_t^T A_{ed}^T}{(1+\beta) + (1-\alpha\beta)P_t^V A_d^V + (1+\beta\gamma)P_t^T A_d^T}$$

$P_t^V$, $P_t^T$ = vector, tensor polarization    $\alpha$, $\beta$, $\gamma$ = normalization ratios

- ✳ Deuteron supports a tensor polarization, $P_t^T$, in addition to the usual vector polarization, $P_t^V$
  - This can lead to both helicity dependent and helicity independent contributions

After (symmetric) acceptance averaging and ignoring small $P_t^T$

$$\epsilon = \frac{1+\alpha\beta}{1+\beta} P_e \, P_t^V A_{ed}^V$$

or

$$A_{ed}^V = \frac{1+\beta}{(1+\alpha\beta) \, P_e \, P_t^V} \epsilon$$

$G_E^n$ extracted via $A_{ed}^V$ from data and MC simulation

## Beam–Target Asymmetry in E93-026

$^{2}\overrightarrow{\mathrm{H}}(\overrightarrow{e}, e'n)p$

$$\sigma(h, P) \approx \sigma_0 \left(1 + hPA_{ed}^{V}\right)$$

$h$: Beam Helicity

$P$: Vector Target Polarization

$T$: Tensor Target Polarization $T = 2 - \sqrt{4 - 3P^2}$

$A_d^T$ is suppressed by $T \approx 3\%$

Theoretical Calculations of electrodisintegration of the deuteron by H. Arenhövel and co-workers

E93-026 $\overrightarrow{\mathrm{D}}(\vec{e}, e'n)p$

$$\sigma(h, P) = \sigma_0 \left(1 + hPA_{ed}^V\right)$$

$A_{ed}^V$ is sensitive to $G_E^n$

has low sensitivity to potential models

has low sensitivity to subnuclear degrees of freedom (MEC, IC)

in quasielastic kinematics

Sensitivity to $G_E^n$ – Insensitivity to Reaction

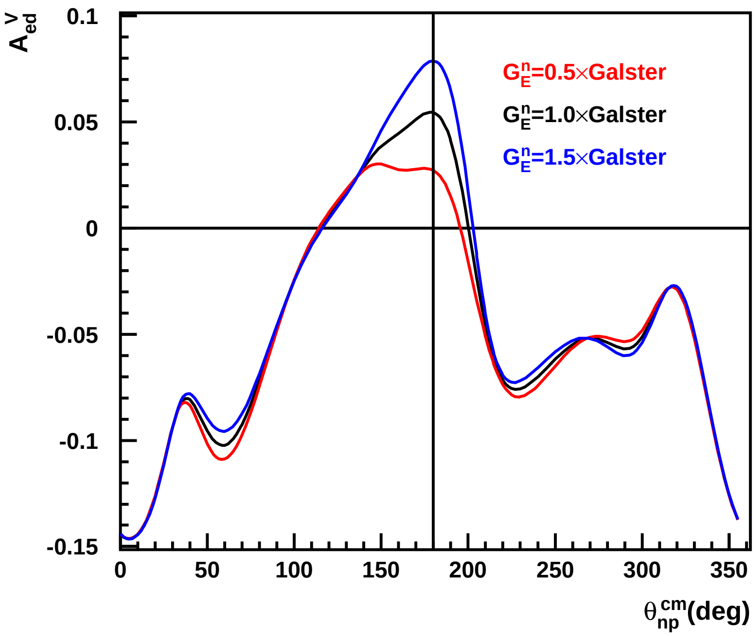


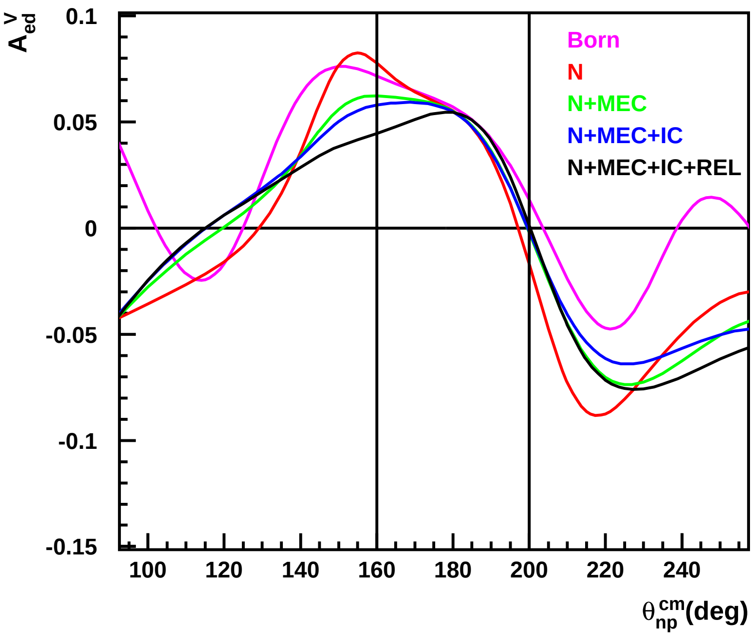

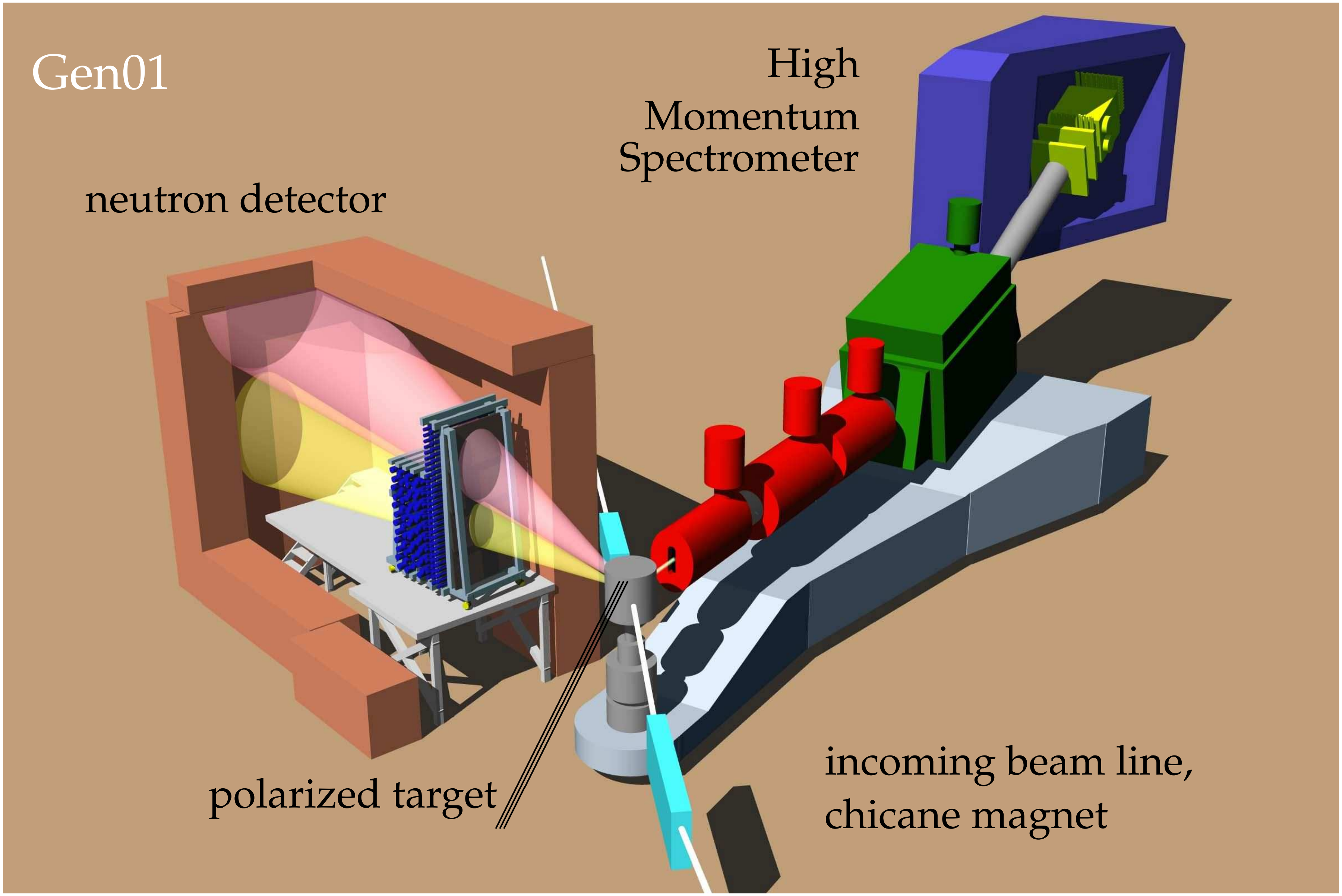
Gen01
High
Momentum
Spectrometer
neutron detector
polarized target
incoming beam line,
chicane magnet

- ✳ Polarized Target
- ✳ Chicane to compensate for beam deflection of $\approx 4$ degrees
- ✳ Scattering Plane Tilted
- ✳ Protons deflected $\approx 17$ deg at $Q^2 = 0.5$
- ✳ Raster to distribute beam over 3 $\mathrm{cm}^2$ face of target
- ✳ Electrons detected in HMS (right)
- ✳ Neutrons and Protons detected in scintillator array (left)
- ✳ Beam Polarization measured in coincidence Möller polarimeter

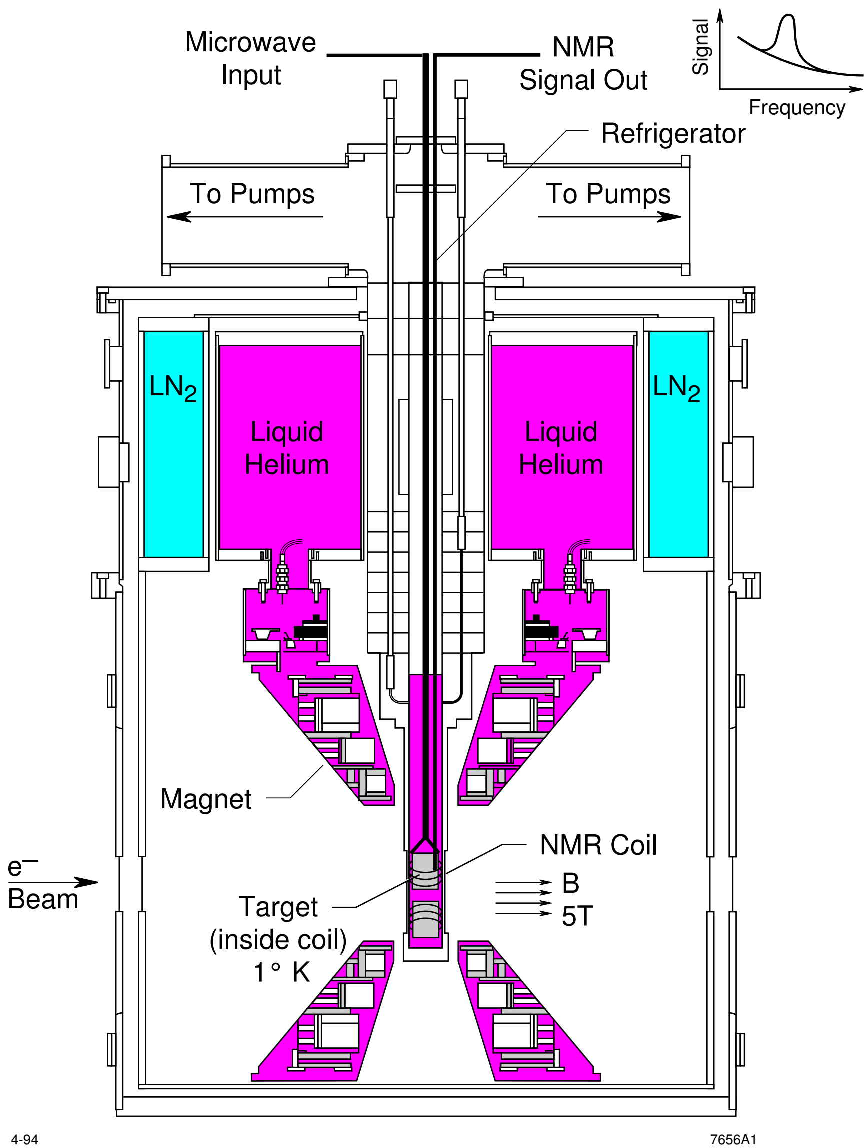


# Solid Polarized Targets

- ✳ frozen(doped) $^{15}ND_3$
- ✳ $^4He$ evaporation refrigerator
- ✳ $5T$ polarizing field
- ✳ remotely movable insert
- ✳ dynamic nuclear polarization

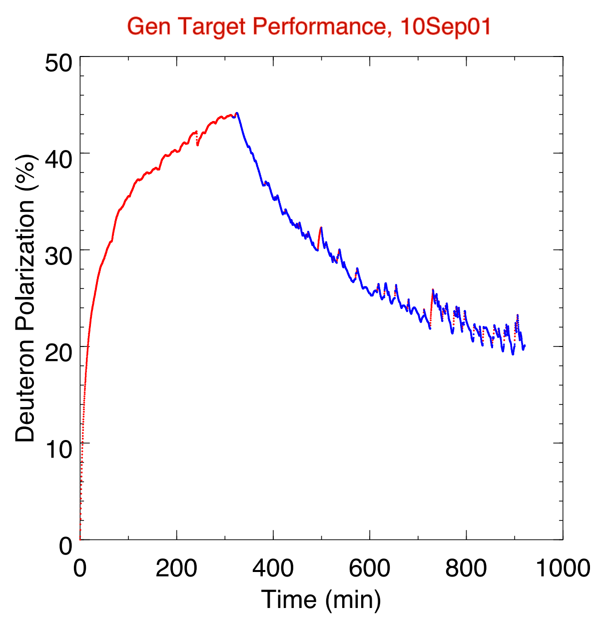

## Neutron Detector

- ✳ Highly segmented scintillator
- ✳ Rates: 50 - 200 kHz per detector
- ✳ Pb shielding in front to reduce background
- ✳ 2 thin planes for particle ID (VETO)
- ✳ 6 thick conversion planes
- ✳ 142 elements total, >280 channels
- ✳ Extended front section for symmetric proton coverage
- ✳ PMTs on both ends of scintillator
- ✳ Spatial resolution $\simeq$ 10 cm
- ✳ Time resolution $\simeq$ 400 ps
- ✳ Provides 3 space coordinates, time and energy

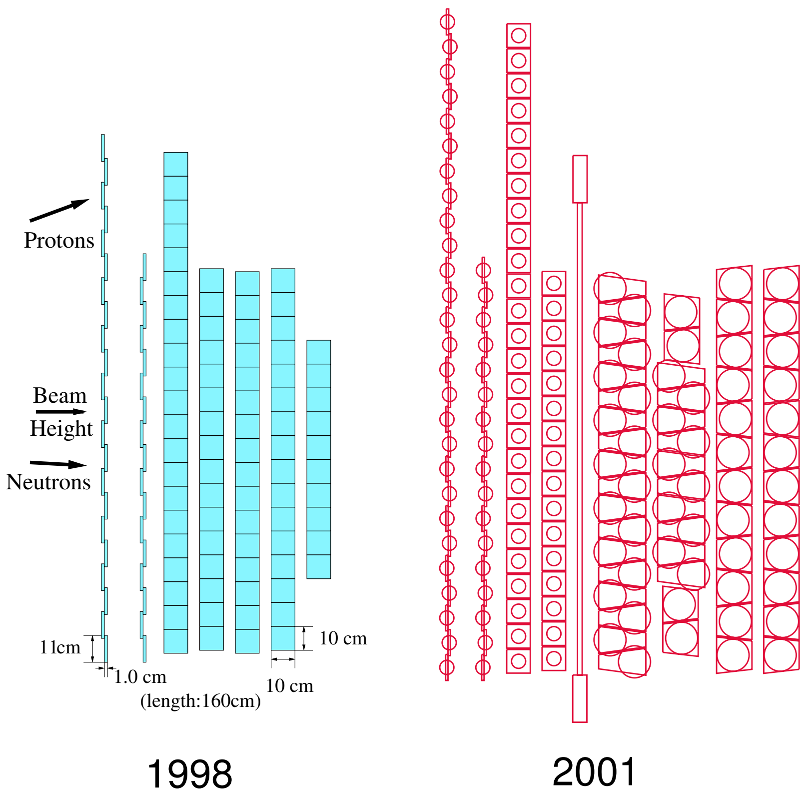


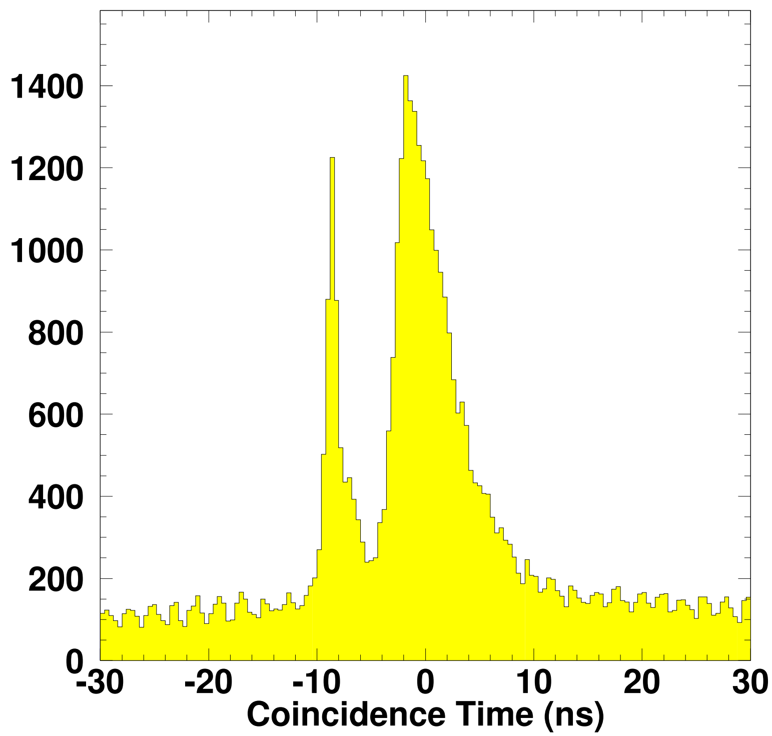

# n Detector — Single Event Display

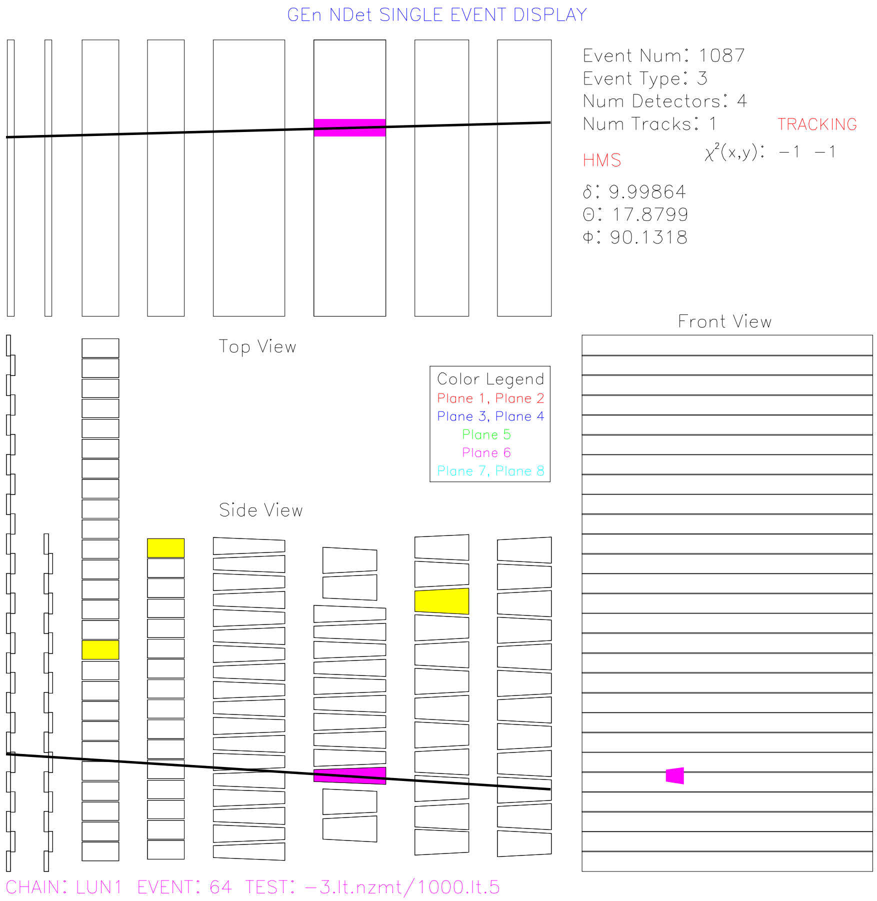


Sample Neutron Track

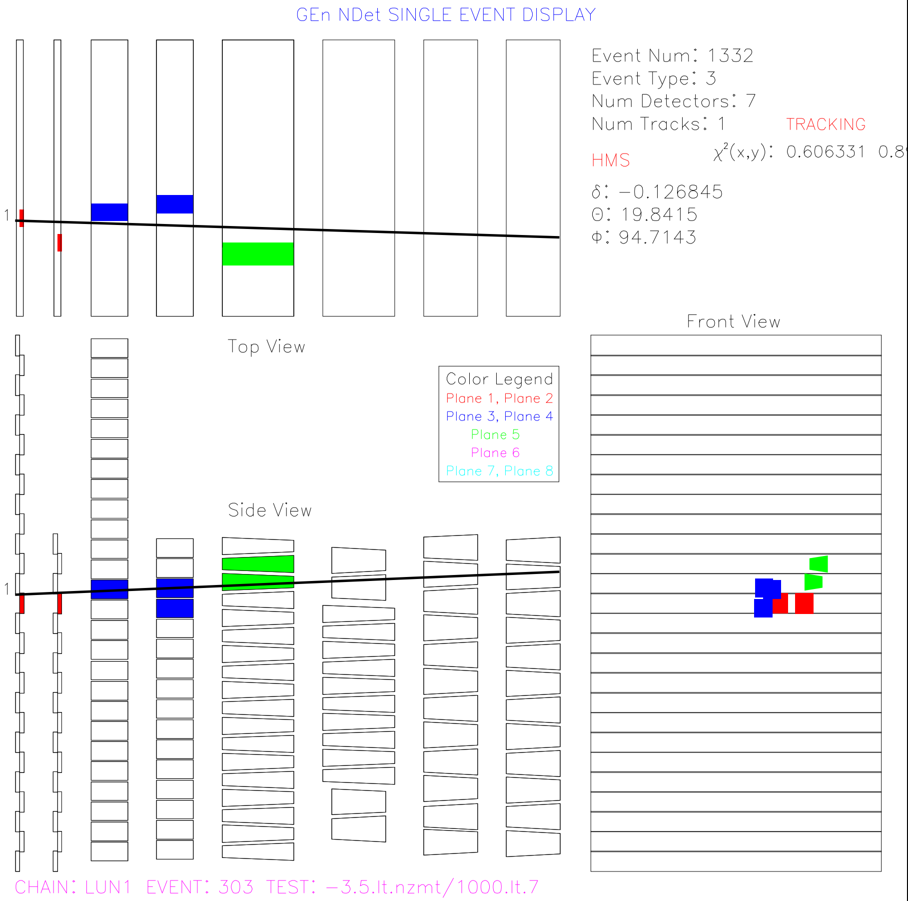


Sample Proton Track

majority of protons in upper half of detector

# Experimental Technique for $\overrightarrow{\mathrm{D}}(\overrightarrow{e}, e'n)p$

For different orientations of $h$ and $P$: $N^{hP} \propto \sigma\,(h, P)$

Beam-target Asymmetry:

$$\epsilon = \frac{N^{\uparrow\uparrow} - N^{\downarrow\uparrow} + N^{\downarrow\downarrow} - N^{\uparrow\downarrow}}{N^{\uparrow\uparrow} + N^{\downarrow\uparrow} + N^{\downarrow\downarrow} + N^{\uparrow\uparrow}} = hPfA_{ed}^{V}$$

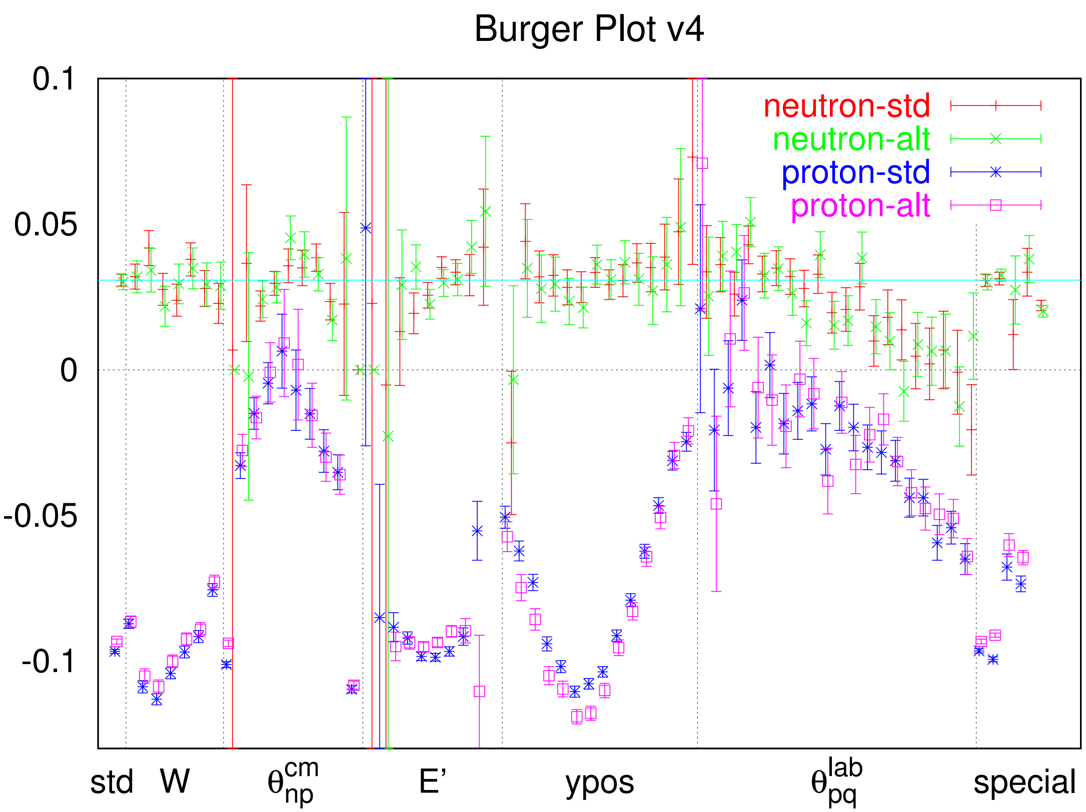

# Data and MC Comparison

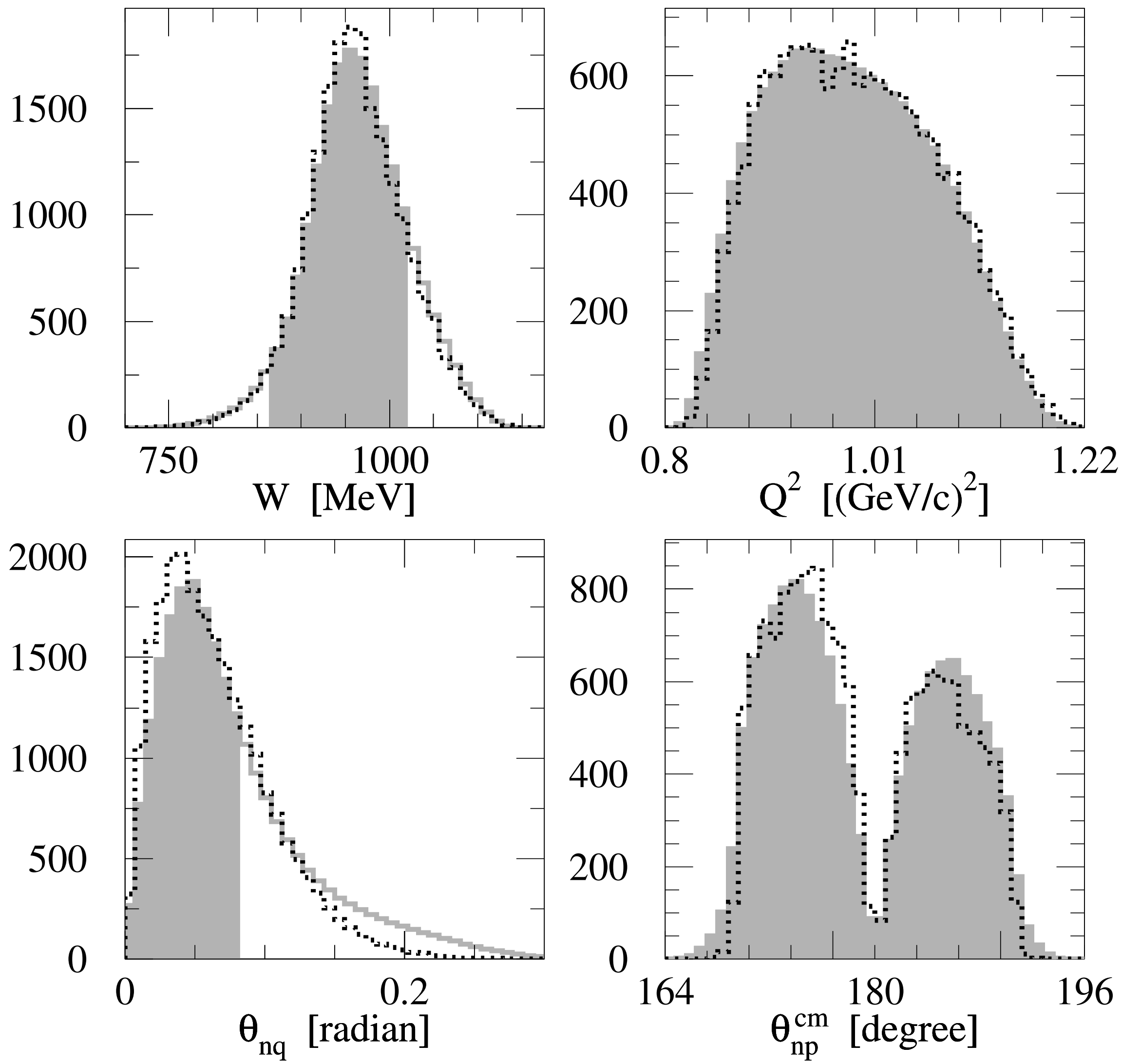

# Extracting $G_E^n$

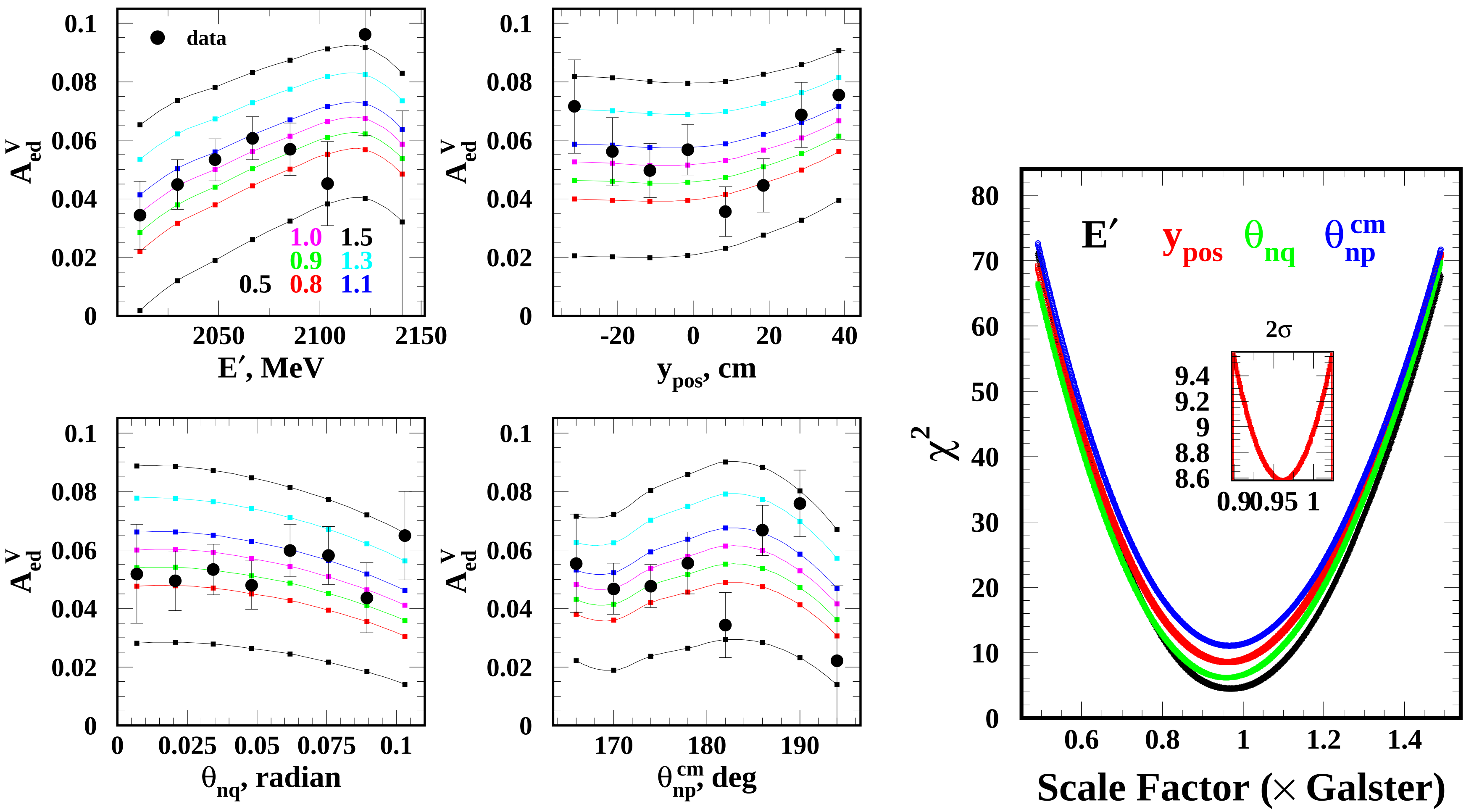

# Results through $\overrightarrow{D}(\vec{e}, e'n)p$

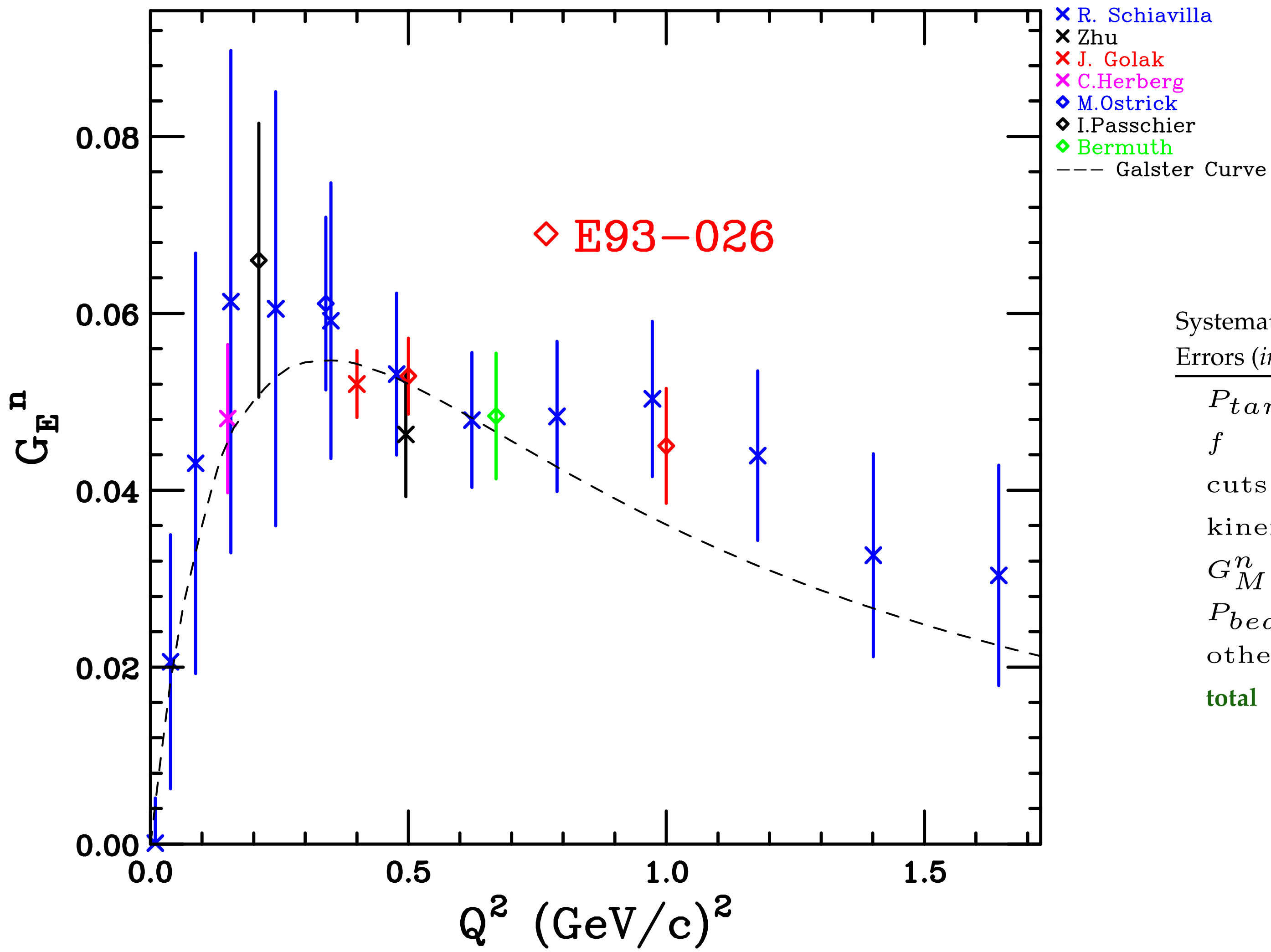


Systematic Errors (*included*):

| | |
|---|---|
| $P_{target}$ | 3-5% |
| $f$ | 3% |
| cuts | 2% |
| kinematics | 2% |
| $G_M^n$ | 1.7% |
| $P_{beam}$ | 1-3% |
| other | 1% |
| **total** | **6-8%** |

# Relevant Theories

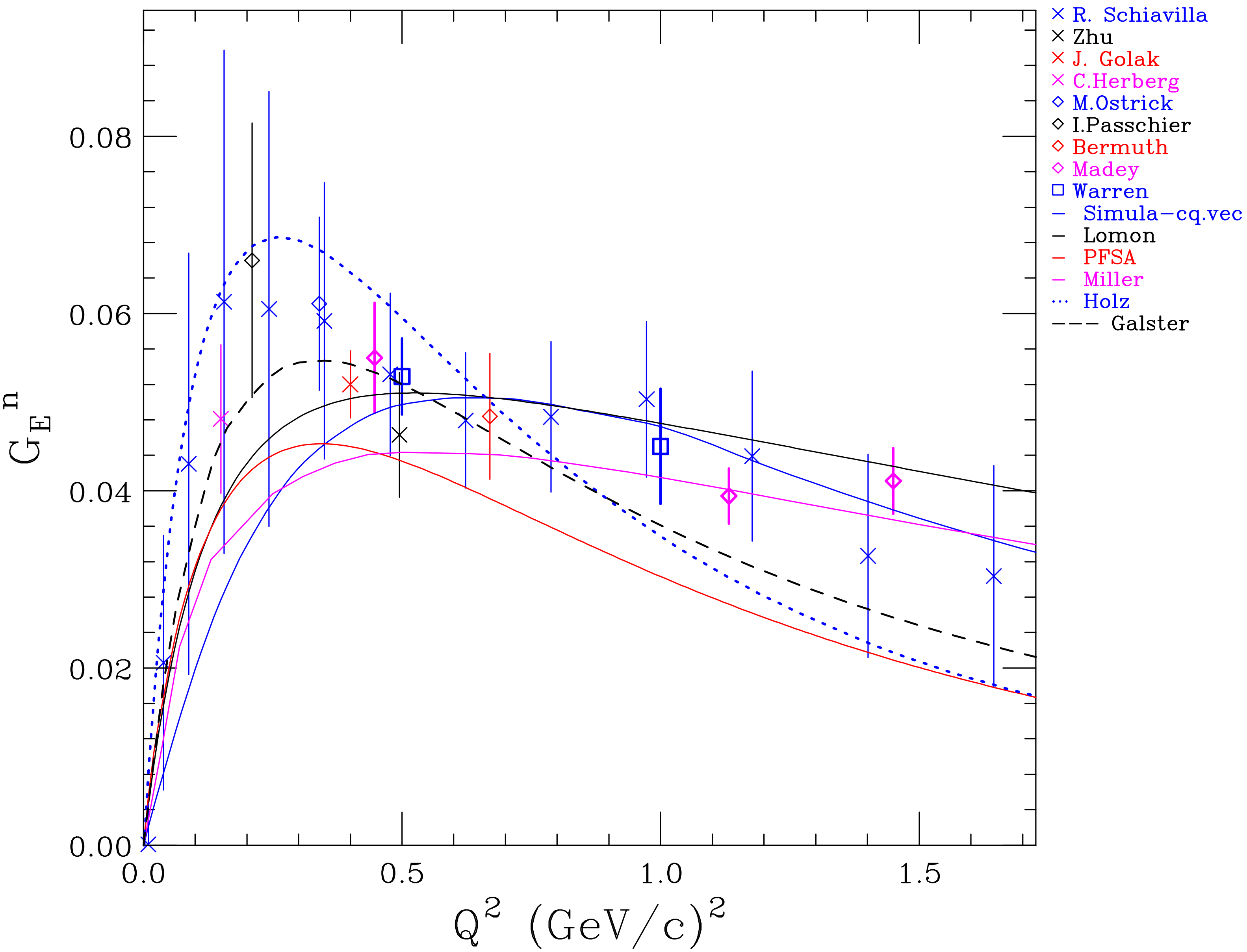

| Laboratory | Collaboration | $Q^2 (GeV/c)^2$ | Reaction | Reported |
|---|---|---|---|---|
| **MIT-Bates** | E85-05 | 0.255 | $^{2}\mathrm{H}(\tilde{e}, e'\tilde{n})$ | 1994 |
| | | $<0.8$ | $^{2}\tilde{\mathrm{H}}(\tilde{e}, e'n)$ | Planned |
| | | $<0.8$ | $^{3}\tilde{\mathrm{He}}(\tilde{e}, e'n)$ | Planned |
| **Mainz-MAMI** | A3 | 0.31 | $^{3}\tilde{\mathrm{He}}(\tilde{e}, e'n)$ | 1994 |
| | A3 | 0.15, 0.34 | $^{2}\mathrm{H}(\tilde{e}, e'\tilde{n})$ | 1999 |
| | A3 | 0.385 | $^{3}\tilde{\mathrm{He}}(\tilde{e}, e'n)$ | 1999 |
| | A1 | 0.67 | $^{3}\tilde{\mathrm{He}}(\tilde{e}, e'n)$ | 1999/2003 |
| | A1 | 0.3, 0.6, 0.8 | $^{2}\mathrm{H}(\tilde{e}, e'\tilde{n})$ | Analysis |
| **NIKHEF** | | 0.21 | $^{2}\tilde{\mathrm{H}}(\tilde{e}, e'n)$ | 1999 |
| **Jefferson Lab** | E93026 | 0.5, 1.0 | $^{2}\tilde{\mathrm{H}}(\tilde{e}, e'n)$ | 2001/2003 |
| | E93038 | 0.45, 1.15, 1.47 | $^{2}\mathrm{H}(\tilde{e}, e'\tilde{n})$ | 2003 |
| | E02013 | 1.3, 2.4, 3.4 | $^{3}\tilde{\mathrm{He}}(\tilde{e}, e'n)$ | Approved |

## Conclusions

- $G_E^n$ remains the poorest known of the four nucleon form factors.
- $G_E^n$ is a fundamental quantity of continued interest.
- Significant progress has been made at several laboratories by exploiting spin correlations
- $G_E^n$ can be described by the Galster parametrization (surprisingly) and data under analysis is of sufficient quality to test QCD inspired models.
- Future progress likely with new experiments and better theory.